

**Metabolic reprogramming of sphingolipids
in the pathogenesis of hepatic adenoma linked to GSD Ia**

Jae Yeon Park

Department of Human Genetics

Faculty of Medicine and Health Sciences

McGill University, Montreal

August, 2023

*A thesis submitted to McGill University in partial fulfillment
of the requirements of the degree of Master of Science*



Abstract

Background: Glycogen storage disease Ia (GSD Ia) is an inherited metabolic disorder characterized by severe hypoglycemia and glycogen accumulation in affected organs. Although dietary therapy has significantly improved metabolic control in GSD Ia, long-term complications such as hepatocellular adenoma (HCA) and chronic kidney inflammation remain common during the second or third decades of life. Recent studies have identified sphingolipid turnover as a hallmark of metabolic disorders, with endogenous sphingolipid profiles continually changing through metabolic reprogramming in conditions such as non-alcoholic fatty liver disease (NAFLD) and diabetic nephropathy. Therefore, we hypothesize that sphingolipids may play a significant role in the pathogenesis of long-term complications in GSD Ia, and this thesis specifically focuses on the liver.

Methods: Using liquid chromatography-tandem mass spectrometry, we developed and validated targeted sphingolipidomic analysis of 20 sphingolipid species from ceramide, sphingomyelin, hexosylceramide, lactosylceramide, sphinganine-1-phosphate and sphingosine-1-phosphate subgroups. Using the developed methods, we constructed sphingolipid profiles of plasma and liver tissue samples obtained from mouse models (wild type $n = 5$, GSD Ia $n = 5$).

Results: The analysis of sphingolipids in GSD Ia mice revealed a significant disturbance in 14 species in plasma and 10 species in liver samples. This variation in the degree of sphingolipid disruptions was found to be dependent on acyl chain length. Furthermore, the compositional analysis indicated that sphingolipid profiles in the plasma and liver displayed distinct

characteristics, suggesting that sphingolipids may exert different functional effects in various physiological and pathological conditions. Of note, the hepatic sphingolipid profiles of 2-week-old GSD Ia mice closely resembled the sphingolipid derangements typically observed in NAFLD, highlighting the potential metabolic overlap between these two disorders.

Conclusions: Significant disruptions in sphingolipid profiles were identified in GSD Ia mouse models, which may be associated with the development of HCA and the progression to cirrhosis later in life. These findings suggest that sphingolipids have the potential to serve as effective biomarkers for monitoring intracellular liver conditions in GSD Ia. Further research is needed to validate the diagnostic and therapeutic implications of sphingolipid metabolism in the long-term pathogenesis of GSD Ia.

Résumé

Contexte: La maladie de stockage de glycogène Ia (GSD Ia) est une maladie métabolique héréditaire caractérisée par une hypoglycémie sévère et une accumulation de glycogène dans les organes affectés. Bien que la thérapie alimentaire ait considérablement amélioré le contrôle métabolique de la GSD Ia, des complications à long terme telles que les adénomes hépatocellulaires (HCA) et l'inflammation rénale chronique restent fréquentes au cours de la deuxième ou troisième décennie de la vie. Des études récentes ont identifié le renouvellement des sphingolipides comme une caractéristique des maladies métaboliques, avec des profils de sphingolipides endogènes en constante évolution par le biais de la reprogrammation métabolique dans des conditions telles que la stéatose hépatique non alcoolique (NAFLD) et la néphropathie diabétique. Par conséquent, nous émettons l'hypothèse que les sphingolipides peuvent jouer un rôle important dans la pathogenèse des complications à long terme de la GSD Ia, et cette thèse se concentre spécifiquement sur le foie.

Méthodes: En utilisant la chromatographie liquide couplée à la spectrométrie de masse en tandem, nous avons développé et validé une analyse ciblée de la sphingolipidomique de 20 espèces de sphingolipides provenant de céramide, sphingomyéline, hexosylcéramide, lactosylcéramide, sphinganine-1-phosphate et sphingosine-1-phosphate. À l'aide des méthodes développées, nous avons construit des profils de sphingolipides d'échantillons de plasma et de tissus hépatiques obtenus à partir de modèles murins de GSD Ia (type sauvage n = 5, GSD Ia n = 5).

Résultats: L'analyse des sphingolipides dans des modèles murins de GSD Ia a révélé une perturbation significative dans 14 espèces dans les échantillons de plasma et 10 espèces dans les échantillons de foie. Cette variation dans le degré de perturbation des sphingolipides dépendait de la longueur de la chaîne acyle. De plus, l'analyse de la composition a indiqué que les profils de sphingolipides dans le plasma et le foie présentaient des caractéristiques uniques, suggérant que les sphingolipides peuvent exercer différents effets fonctionnels dans diverses conditions physiologiques et pathologiques. À noter, les profils sphingolipidiques hépatiques des souris atteintes de GSD Ia de 2 semaines ressemblaient étroitement aux anomalies sphingolipidiques observées typiquement dans la NAFLD, soulignant encore l'importance des sphingolipides dans la pathogenèse hépatique.

Conclusions: Des perturbations significatives des profils de sphingolipides ont été identifiées chez les modèles de souris atteints de GSD Ia, qui peuvent être associées au développement de HCA et à la progression vers la cirrhose plus tard dans la vie. Ces résultats suggèrent que les sphingolipides ont le potentiel de servir de biomarqueurs efficaces pour surveiller les conditions intracellulaires du foie dans le GSD Ia. Des recherches supplémentaires sont nécessaires pour valider ces résultats et explorer les implications diagnostiques et thérapeutiques potentielles.

Table of Contents

ABSTRACT	2
RÉSUMÉ	4
TABLE OF CONTENTS	6
LIST OF ABBREVIATIONS	9
LIST OF FIGURES.....	11
LIST OF TABLES.....	12
ACKNOWLEDGEMENTS	13
ACKNOWLEDGEMENTS - FUNDING	14
CONTRIBUTION OF AUTHORS	15
CHAPTER 1. INTRODUCTION.....	16
1.1 HEPATIC GLYCOGEN STORAGE DISEASE	16
1.1.1 GLYCOGEN STORAGE DISEASE TYPE IA	16
1.1.2 HEPATOCELLULAR ADENOMA IN GSD IA.....	20
1.2 SPHINGOLIPIDS.....	22
1.2.1 SPHINGOLIPID METABOLISM.....	22
1.2.2 EXPLORING THE MECHANISMS OF CERAMIDE-INDUCED LIPOTOXICITY IN CELLS	26
1.2.3 SPHINGOLIPIDS AND METABOLIC DISORDERS	28
1.3 LIQUID CHROMATOGRAPHY COUPLED WITH TANDEM MASS SPECTROMETRY	30
1.3.1 LIQUID CHROMATOGRAPHY (LC).....	31
1.3.2 TANDEM MASS SPECTROMETRY (MS/MS)	33
1.4 OBJECTIVE OF THE STUDY	36

1.4.1 PRIMARY OBJECTIVE.....	36
1.4.2 SPECIFIC STUDY AIMS	37

CHAPTER 2. METHODOLOGY38

2.1 MATERIALS AND METHODS	38
2.1.1 MATERIALS	38
2.1.1.1 Standards and solvents.....	38
2.1.1.2 Internal standards.....	38
2.1.1.3 Preparation of standard solution	39
2.1.2 BIOLOGICAL SAMPLES	39
2.2 SPHINGOLIPID EXTRACTION	40
2.3 QUALITY CONTROL	41
2.4 CARRYOVER	41
2.5 METHOD VALIDATION.....	41
2.5.1 LINEARITY	42
2.5.2 PRECISION AND ACCURACY	42
2.5.3 RECOVERY	43
2.5.4 REPRODUCIBILITY	43
2.6 STATISTICS	43

CHAPTER 3. RESULTS 1 – METHOD DEVELOPMENT AND VALIDATION44

3.1 SPHINGOLIPID EXTRACTION	45
3.1.1 LIQUID-LIQUID EXTRACTION METHOD.....	46
3.1.2 SINGLE-PHASE EXTRACTION METHOD	48
3.2 LC-MS/MS CONDITIONS	48
3.2.1 LC SEPARATION CONDITIONS	48
3.2.1.1 Ceramide and complex sphingolipids.....	48
3.2.1.2 Phosphate sphingolipids	49
3.2.2 INTELLISTART™	50
3.3 METHOD VALIDATION.....	52
3.3.1 CERAMIDE AND COMPLEX SPHINGOLIPIDS	52
3.3.2 PHOSPHATE SPHINGOLIPIDS	52
3.4 QUANTIFICATION OF SPHINGOLIPIDS IN QC SAMPLES	55

CHAPTER 4. RESULTS 2 – TARGETED SPHINGOLIPIDOMICS IN GSD IA MICE...58

4.1 ELEVATED SPHINGOLIPID LEVELS IN GSD IA MICE PLASMA	58
4.2 HEPATIC SPHINGOLIPID METABOLISM IN GSD IA MICE.....	60
4.3 DISTURBED SPHINGOLIPID PROFILES IN GSD IA MOUSE PLASMA AND LIVER	61
<u>CHAPTER 5. DISCUSSION 1: GSD IA AND NAFLD.....</u>	<u>63</u>
<u>CHAPTER 6. DISCUSSION 2: SPHINGOLIPID PROFILES</u>	<u>67</u>
<u>CHAPTER 7. FUTURE DIRECTIONS.....</u>	<u>70</u>
7.1 SPHINGOLIPIDS CHANGEOVER ALONG THE GSD IA PROGRESSION.....	70
7.2 SPHINGOLIPIDS CHANGEOVER IN GSD IA-KIDNEYS	71
7.3 PHARMACOLOGICAL INTERVENTIONS IN SPHINGOLIPID METABOLISM	72
<u>CHAPTER 8. CONCLUSION</u>	<u>74</u>
<u>REFERENCES</u>	<u>77</u>
<u>APPENDICES: SUPPLEMENTAL INFORMATION.....</u>	<u>83</u>

List of Abbreviations

Akt	Protein kinase B
Apo	Apolipoprotein
ATP	Adenosine triphosphate
CD36	Cluster of differentiation 36
Cer	Ceramide
CerS	Ceramide synthase
CERT	Ceramide transfer protein
COX-2	Cyclooxygenase-2
CV	Coefficient of variation
CVD	Cardiovascular disease
C1P	Ceramide-1-phosphate
DhCer	Dihydroceramide
ER	Endoplasmic reticulum
ESI	Electrospray ionization
ETC	Electron transport chain
FDA	The United States Food and Drug Administration
GluCer	Glucosylceramide
GLUT	Glucose transporter
GSD	Glycogen storage disease
G6P	Glucose 6-phosphate
HCA	Hepatocellular adenoma
HCC	Hepatocellular carcinoma
HDL	High-density lipoprotein
HexCer	Hexosylceramide
IL	Interleukin

IS	Internal standard
LacCer	Lactosylceramide
LC	Liquid chromatography
LC-MS/MS	Liquid chromatography tandem mass spectrometry
LDL	Low-density lipoprotein
LOD	Limit of detection
LOQ	Limit of quantification
MRM	Multiple-reaction monitoring
MS	Mass spectrometry
NaCl	Sodium chloride
NADPH	Nicotinamide adenine dinucleotide phosphate
NAFLD	Non-alcoholic fatty liver disease
NASH	Nonalcoholic steatohepatitis
NF- κ B	Nuclear factor kappa-light-chain-enhancer of activated B cells
PKC ζ	Protein kinase C, zeta
PP2A	Protein Phosphatase 2A
QC	Quality control
RE	Relative error
ROS	Reactive oxygen species
RT	Retention time
Sa1P	Sphinganine-1-phosphate
SM	Sphingomyelin
SMase	Sphingomyelinase
S1P	Sphingosine-1-phosphate
TBS	Tris-buffered saline
TFA	Trifluoroacetic acid
T2D	Type 2 Diabetes
VLDL	Very low-density lipoproteins

List of Figures

- Figure 1** A schematic representation of the glucose-6-phosphatase system
- Figure 2** Disturbed glucose metabolism in GSD Ia liver and kidneys
- Figure 3** Summarized pathway of sphingolipid metabolism
- Figure 4** Sphingolipid biosynthesis and transport
- Figure 5** Ceramide-dependent lipotoxicity
- Figure 6** Reversed-phase chromatography elution
- Figure 7** Scheme of tandem mass spectrometry
- Figure 8** Typical MS/MS fragmentation patterns of sphingolipids
- Figure 9** Amphipathic sphingolipids
- Figure 10** Illustration of sphingolipid extraction protocols
- Figure 11** Chromatographic gradient used for sphingolipid separation.
- Figure 12** Chromatographic separation of phosphate sphingolipids from extracted QC sample
- Figure 13** The measured concentration of phosphate sphingolipids in QC samples using single-phase extraction and targeted sphingolipidomic methods
- Figure 14** Compositional analysis representing the abundance of sphingolipids in (A) mouse plasma and (B) mouse liver tissue.
- Figure 15** FDA-approved drugs targeting sphingolipid metabolizing enzymes
- Figure S1** Chromatographic separation of sphingolipids by targeted sphingolipidomics using LC-MS/MS

List of Tables

Table 1	General composition of lipoproteins and distribution of circulating sphingolipids.
Table 2	Overview of extraction and LC methods according to the type of sphingolipids
Table 3	MRM transitions and optimized parameters for each analyte
Table 4	Validation parameters in LC-MS/MS: linearity, reproducibility, recovery, intra- and inter-day precision, intra- and inter-day accuracy, LOQ and LOD
Table 5	The comparison of sphingolipid concentrations in mouse plasma
Table 6	The comparison of sphingolipid concentrations in mouse plasma
Table 7	Sphingolipid Perturbation in Mouse Hepatocytes: A Comparison between GSD Ia and NAFLD
Table S1	Sphingolipid species information and molecular structure
Table S2	Lipid standards and stock solutions

Acknowledgements

After a long and unforgettable journey, I have finally come to the end of my project, and I would like to take this opportunity to express my sincere gratitude to all those who have contributed to its success.

First and foremost, I would like to express my deepest appreciation to my supervisor, Dr. John J. Mitchell, for giving me the invaluable opportunity to work on rare disorders. Studying metabolic disorders has been a lifelong dream of mine, and it is thanks to him that I was able to make this dream a reality. At every stage of the project, I benefited from his kind advice and support, which helped me develop as a researcher in the best possible way. I have always held him in high regard not just as a skilled professor but also as a remarkable individual.

I would like to thank my supervisory committee member, Dr. Najma Ahmed, for her valuable suggestions during each committee meeting. I would like to extend a special mention to Dr. Farah El Turk for sharing her knowledge of analytical chemistry with me. Her constructive criticism has enabled me to develop a strong understanding of biochemistry, in addition to my background in biology.

I feel incredibly fortunate to have received invaluable assistance from a variety of experts at the MUHC. I would like to express my sincere gratitude to Dr. Karen Elizabeth Christensen for her exceptional help with method development, and for generously sharing her wholehearted advice and knowledge. I would also like to acknowledge the priceless aid and guidance provided by Dr. Mohammed Kaouache, who willingly shared his time and expertise on statistical analysis with our team. Their support has been instrumental in the success of my

work, and I am deeply grateful for their contributions. Furthermore, I would like to express my appreciation to Dr. Koeberl's team, our collaborators, for providing all mouse samples and relevant information. I would like to thank all members of Dr. Mitchell's team including Ms. Moisan, Ms. Younglai, Eric, Karine and Yeniay.

Finally, my heartfelt appreciation goes out to all my friends and colleagues at the MUHC. Over the past two years, navigating the challenges of a master's program has been an unexpected journey. However, they listened to my concerns more seriously than anyone else, advised me, and worked hard to find solutions. It was a great privilege and honor for me to work and study in the MUHC.

Dear beloved husband and family, I am humbled and deeply grateful for your utmost love and support that has been the driving force behind my success. I owe my achievements to your unwavering dedication and countless sacrifices, without which I would not be where I am today. You have been my rock and my true home, providing a safe haven where I can rest and rejuvenate my mind. I feel incredibly blessed to have the most caring and loving family in the world. Thank you, my heroes.

Acknowledgements - Funding

This study received partial support from the RI-MUHC Desjardins Studentship Awards, Isaac Foundation, and Harpur Foundation. The research grant and studentship provided by these esteemed institutions and foundations enabled the successful execution of this study, and I extend my sincere gratitude to them for their invaluable support.

Contribution of Authors

This thesis manuscript was produced through the collaborative efforts of the listed authors, who contributed to various stages of designing, experimentation, research, and writing. Jae Yeon Park, the first author, conducted the experiments, optimized the methods, interpreted the results, and composed all chapters of this dissertation. Dr. John J. Mitchell served as the principal investigator of this project and developed the main research questions, supervised the overall project, and participated in the revisions, review and submission of the manuscript. Dr. Farah El Turk played a critical role in project management, directing the experimental process and revising and reviewing the manuscript. Dr. Mohammed Kaouache conducted all of the statistical analyses and provided valuable statistical advice for this study. Dr. Dwight Koeberl and his research team provided all mouse samples utilized in this project, as well as the corresponding sources. Dr. Karen Elizabeth Christensen offered valuable guidance during the method development process, particularly in the successful execution of liver tissue experiments. Members of Dr. Mitchell's research lab, Karine Bernier and Yeniay Erdem, contributed to this project through their involvement in the experiments. All authors declared no conflict of interest regarding this manuscript.

CHAPTER 1. INTRODUCTION

1.1 Hepatic glycogen storage disease

1.1.1 Glycogen storage disease type Ia

Glycogen storage disorder type I (GSD I), also known as Von Gierke disease, is an autosomal recessive genetic disorder caused by enzyme deficiencies in glycogen metabolism (1). GSD I was first described by Von Gierke in 1929, who observed excessive accumulation of hepatic and renal glycogen in the autopsy reports of two children (1). In 1952, Cori and Cori demonstrated that this disorder was caused by a deficiency in glucose-6-phosphatase (G6Pase) enzyme activity, representing a significant milestone in the understanding of GSD I as a metabolic disorder affiliated with enzyme defects (2). Today, this specific form of GSD I is known as GSD Ia. In 1978, Narisawa *et al.* discovered that some GSD I patients had normal G6Pase activity but were unable to degrade G6P *in vivo* (3). Investigation into this group of patients showed that they had a defect in the G6P transport system, which resulted in the inability of G6P molecules to be transported into the lumen of the endoplasmic reticulum for enzymatic metabolism (**Figure 1**). This subgroup was classified as GSD Ib, which helped broaden the classification of GSD I based on specific defects. Subsequent studies by Arion *et al.* identified a multi-component enzyme system associated with G6Pase, where deficiencies in specific components resulted in different subgroups of GSD I (**Figure 1**) (2). Due to the distinct pathogenesis observed among subgroups of GSD I, this study specifically focused on GSD Ia.

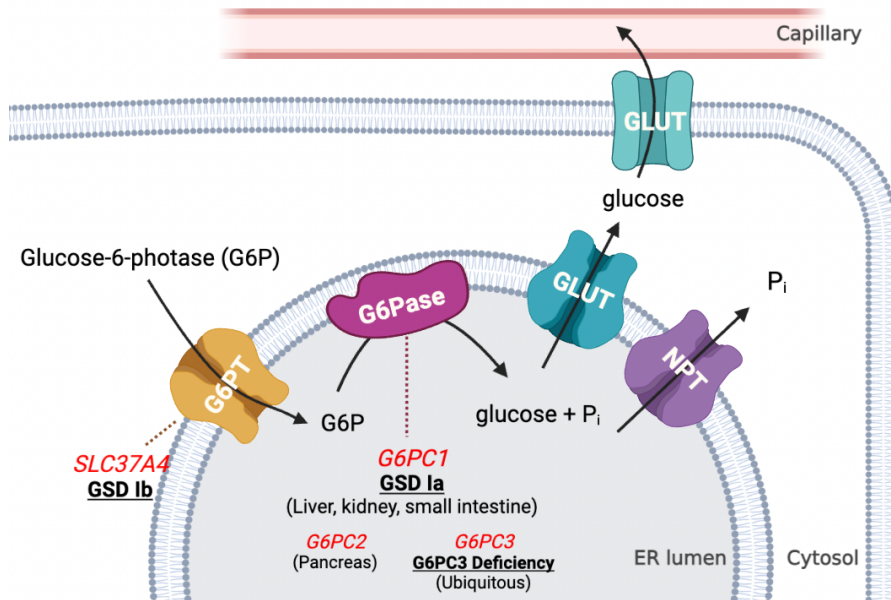


Figure 1. A schematic representation of the glucose-6-phosphatase system

Genes are displayed in red font and the expression sites of the genes are presented in bold white font.

The human *G6PC* gene encodes the catalytic subunit of G6Pase (**Figure 1**) (4). This enzyme involves the final step of both glycogenolysis and gluconeogenesis by hydrolyzing G6P and releasing the free glucose into the bloodstream (5). Mutations in the *G6PC1* cause a G6Pase deficiency which leads to GSD Ia, accounting for around 80 % of the total GSD I case (2).

Due to the deficiency of the G6Pase enzyme, GSD Ia patients exhibit impaired gluconeogenesis in the liver and kidneys (**Figure 2**) (4). In GSD Ia, G6P cannot be catalyzed to free glucose in hepatocytes and renal cells, leading to severe hypoglycemia during short-term fasting (5). The undegraded G6P in the cytoplasm stimulate alternative pathways resulting in hypercholesterolaemia, hypertriglyceridemia, hyperuricaemia and hyperlactataemia (4). In addition, excess G6P can trigger the accumulation of fat and glycogen, which can be fatal to hepatocytes and renal cells (**Figure 2**) (4).

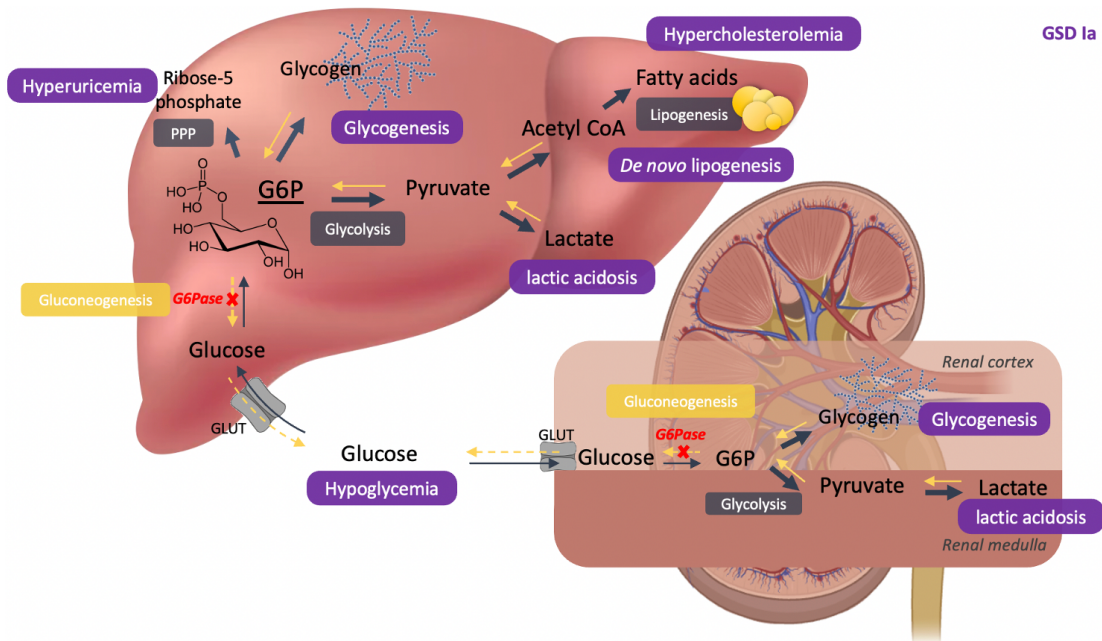


Figure 2. Disturbed glucose metabolism in GSD Ia liver and kidneys

The clinical presentation of GSD Ia can vary between cases, but the average age of diagnosis is around 27.6 months (6). During the neonatal period, patients with GSD Ia may present feeding difficulties, seizures, irritability, and somnolence due to hypoglycemia and lactic acidosis (7, 8). These symptoms can be shared with other metabolic diseases, making an accurate diagnosis of GSD Ia challenging and potentially delayed in pediatric patients. As patients age, clinical symptoms become more apparent, including doll-like faces, hepatomegaly, delayed development, and growth retardation (4). In 2002, a well-organized retrospective study on GSD I was published (8). This study analyzed 288 GSD I patients (including both GSD Ia & Ib) and identified hepatocellular adenoma (HCA) and progressive renal disease as major causes of mortality in these patients (8).

GSD Ia patients are at a heightened risk of recurrent hypoglycemia, emphasizing the importance of maintaining blood glucose levels within the normal range (4). To this end,

uncooked cornstarch is a vital component of the dietary treatment plan, as it prolongs carbohydrate absorption from the gastrointestinal tract and extends periods of normoglycemia between feeds (8). Adult patients require less glucose; thus, they can substitute cornstarch with a high-complex-carbohydrate snack during the day. Minimizing acidosis is also a critical aspect of managing the hepatic GSD Ia (9). Dietary sucrose, fructose, and galactose are recommended to be limited for GSD Ia patients as these sugars cannot be metabolized, leading to elevated lactate concentrations and acidosis (10). Although there is no precise threshold determined to date for sugar levels that trigger biochemical abnormalities in GSD Ia patients, it is advised that non-utilizable sugar consumption is kept to less than 2.5 grams per meal for optimal metabolic conditions (10). This means that patients should restrict their intake of fruits and sweetened beverages with high amounts of fructose, milk and dairy products that contain high concentrations of lactose, as well as certain vegetables which may contain high levels of galactose (10). Given the stringent dietary restrictions, GSD Ia patients are prescribed supplements and multivitamins, specifically vitamin D and calcium to meet their nutritional requirements (9).

Over the past few decades, significant progress has been made in the metabolic control of GSD Ia, leading to a substantial improvement in the life expectancy of patients with GSD Ia (2). Nevertheless, long-term complications, including HCA with the potential of secondary formation to hepatocellular carcinomas continue to occur frequently in adolescent and adult patients (3). Therefore, it is highly recommended to perform regular surveillance of liver and kidney functions for GSD Ia patients after the onset of puberty (3).

1.1.2 Hepatocellular adenoma in GSD Ia

As many GSD Ia patients reach adulthood, the risk of long-term complications such as progressive liver diseases became a significant burden for survivors (11, 12). HCA formation is one of the most notable complications associated with GSD Ia, particularly in post-pubertal patients. In addition, malignant transformation to hepatocellular carcinoma (HCC) has been reported in several cases (8). A retrospective study conducted on GSD I patients (including both GSD Ia & Ib) has shown that 56.9 % of participants developed HCA at an age range of 7.9 – 26.3 years with 75 % of cases occurring during or after puberty (12). Among the GSD I patients with HCA, 13.8 % of cases progressed further to HCC (12).

Moreover, managing GSD Ia-HCA is particularly challenging due to the lack of effective tools for accurate precision, prevention, and monitoring of disease progression. Although several studies have highlighted the potential for adenoma sizes to progress and malignant transformation to occur with age in individuals with GSD Ia, clinical research on developing specific biomarkers for this matter is still lacking (9, 13). While excessive glycogen deposition is a common secondary biochemical abnormality in hepatic-GSD, GSD Ia has been shown to have a predominantly higher risk of developing HCA compared to other types of GSD (11). The regulatory mechanism of adenoma development in hepatic-GSD remains unknown, and the reasons for the higher risk of HCA in GSD Ia patients are not yet clearly identified.

Some studies have suggested that metabolic imbalances may play a role in HCA development, but these findings remain controversial (11, 14). During adolescence, there has been a noticeable surge in the incidence of HCA in GSD Ia, which could be attributed to suboptimal metabolic control during this period as well as the secretion of pubertal hormones (5, 9, 15). A recent study found a significant correlation between the development of HCA and

mean serum triglyceride levels, underscoring the importance of implementing intensive dietary treatment to prevent HCA development (15). However in another case-control study, no significant differences were observed in metabolic parameters between GSD Ia patients who developed HCA and those who did not (16).

The rarity of GSD Ia poses a significant challenge in obtaining a sufficient sample size for research, which is necessary to achieve robust and conclusive results. In addition, GSD Ia is a heterogeneous disease, with variations in clinical presentation and severity, making it complex to draw definitive inferences that cover the full spectrum of the disease (17). These factors contribute to the practical limitations in studying the long-term complications of GSD Ia and emphasize the need for collaborative efforts and multi-center research to advance our understanding of the disease.

1.2 Sphingolipids

1.2.1 Sphingolipid metabolism

All eukaryotic cells are encased in a plasma membrane, which serves as a barrier between the cell's interior and the external environment while also playing an active role in intercellular communication (18). One key structural component of the plasma membrane is sphingolipids and their metabolites (18).

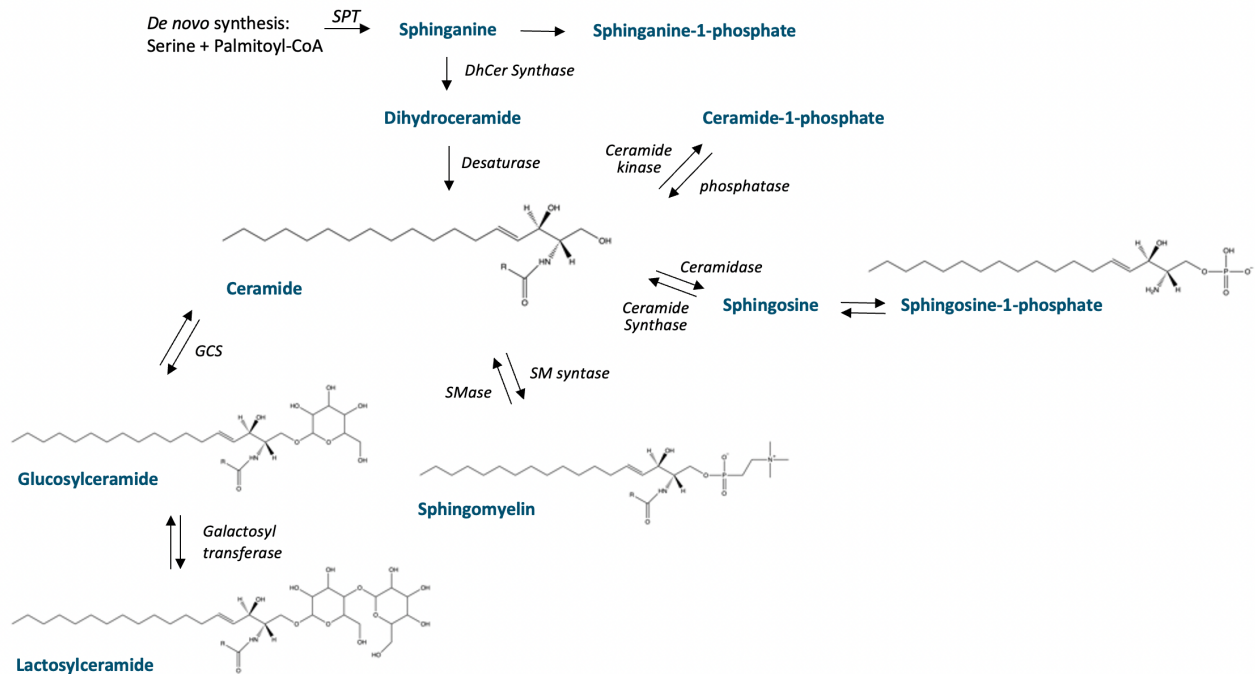


Figure 3. Summarized pathway of sphingolipid metabolism

Sphingolipids are composed of a common sphingosine/sphinganine backbone, which can be modified by acylation, glycosylation, phosphorylation, and linkage to polar head groups, giving rise to a diverse range of subtypes (**Figure 3**) (19). This structural diversity is directly

linked to their functional diversity, which enables sphingolipids to perform unique and essential roles in both intra- and extracellular signaling pathways (19).

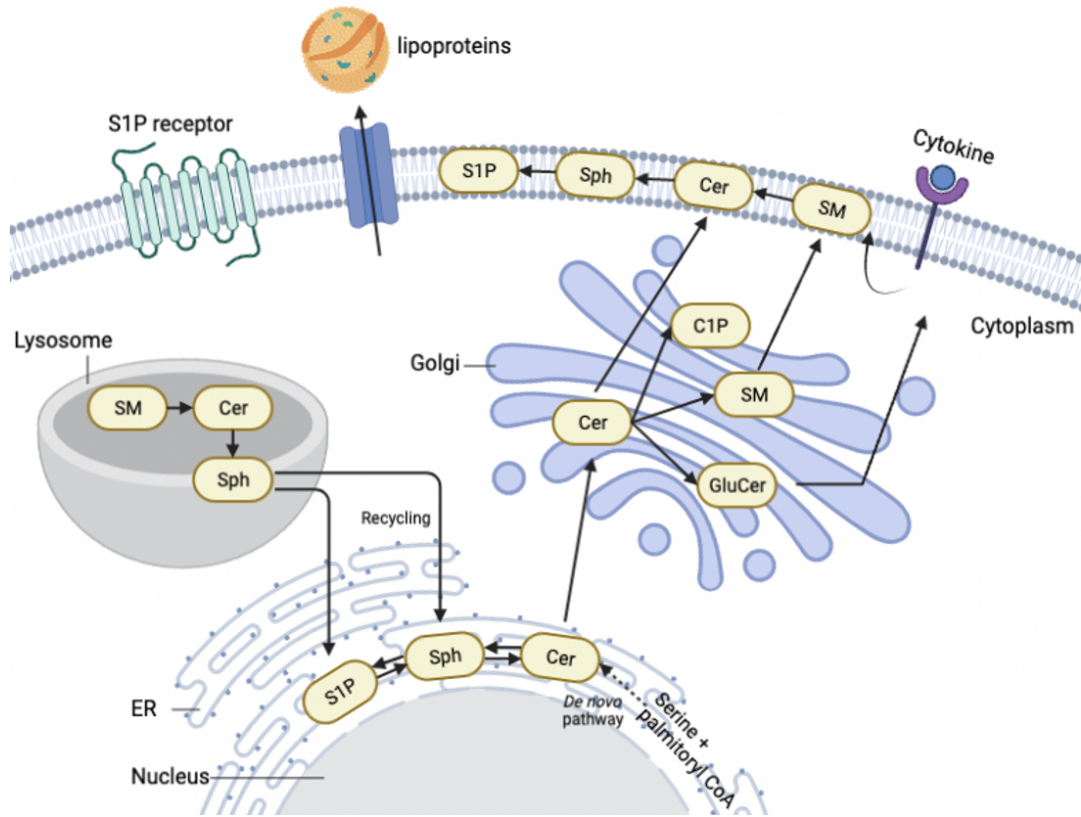


Figure 4. Sphingolipid biosynthesis and transport

De novo synthesis of sphingolipid metabolism starts with the condensation of palmitoyl-CoA and serine in the endoplasmic reticulum which leads to the production of sphinganine and subsequently, ceramide (**Figure 4**) (20). During this synthesis, a family of six ceramide synthase isoforms (CerS1- CerS6) involves differing preferences for specific acyl chain lengths (18). CerS1 solely uses 18 carbon (C18) acyl CoA to the sphingoid base; CerS2 attaches very-long fatty acyl chains, forming C22-C24 Ceramide; CerS4 synthesizes C18–C20 ceramide; and CerS5 and 6 prefer C14–C16 fatty acyl CoA (18). Ceramide is then transported to the Golgi apparatus

where it is converted into complex sphingolipids such as ceramide-1-phosphate (C1P), sphingomyelin (SM), and glucosylceramide (GluCer) (**Figure 4**) (21). In addition to *de novo* synthesis, ceramides can also be generated from the hydrolysis of sphingomyelin or the conversion of other complex sphingolipid metabolites (18). These reactions are reversible, and the concentrations of each species dynamically adjust through a reprogramming of sphingolipid metabolism in order to maintain intracellular homeostasis (22). Mature sphingolipids are carried to the plasma membrane, particularly lipid rafts which are specialized regions that serve as a reservoir for sphingolipids and cholesterol (**Figure 4**) (23). These lipid-rich domains play a critical role in regulating a variety of cellular functions, including signal transduction, receptor trafficking, responses to pathogens and cytokines and membrane fluidity (23). By concentrating sphingolipids and cholesterol within lipid rafts, cells can fine-tune their membrane properties and create specialized microenvironments for specific cellular processes (24). Sphingolipids can remain in the cellular membrane or can also be transported to lipoproteins and albumin for distribution throughout the body (**Figure 4, Table 1**) (25, 26).

	VLDL	LDL	HDL	Total
Sphingolipid composition				
Sphingomyelins	3 - 7 %	33 - 50 %	43 - 64 %	100 %
Ceramides	9 - 16 %	40 - 60 %	24 - 51 %	100 %
Glycosphingolipids	6 - 9 %	42 - 50 %	42 - 52 %	100 %
Sphingosine-1-phosphates	1 - 2 %	4 - 6 %	90 - 95 %	100 %
Apoprotein				
Type of apoprotein	Apo B-100, Apo E, Apo C	Apo B-100	Apo A, Apo C, Apo E	

* Percentage of total content carried by circulating lipoproteins

Table 1. General composition of lipoproteins and distribution of circulating sphingolipids. The table is adapted from Le Barz *et al.* (26)

Lipoproteins are the main carrier of circulating sphingolipids. Ceramides, which constitute about 3 % of plasma sphingolipids, are primarily distributed among apoB-containing lipoproteins (**Table 1**) (25, 26). A paper published by Iqbal *et al.* found that apo-B lipoproteins are responsible for 90 % of the circulating ceramide (25). This discovery is significant because ceramide is present in all cells, but circulating ceramides are mainly influenced by apo-B lipoproteins. Based on the fact that apo-B lipoproteins are predominantly synthesized and released from the liver, it can be inferred that hepatic and enterocytic ceramides are primarily destined for secretion to other tissues (25, 26).

Sphingomyelin is the most abundant subgroup in the plasma sphingolipid profile, accounting for about 90 % of the total plasma sphingolipids (25-27). Chylomicrons and very low-density lipoproteins (VLDL) are the primary carriers of sphingomyelin in circulation, with approximately 57 % of sphingomyelin being circulated in these lipoproteins (**Table 1**) (26, 27). Sphingosine-1-phosphate (S1P) is another important sphingolipid that is relatively more abundant in plasma than in tissues (28). In normal conditions, S1P is predominantly found in albumin (30 ~ 40 %) and high-density lipoproteins (HDL, 50 ~ 60 %) with very little on LDL or VLDL (25, 26, 28). However, there is limited knowledge regarding the secretion and synthesis of sphingolipids in lipoproteins, necessitating further research to elucidate the detailed mechanisms and pathways of circulating sphingolipids.

Once in the extracellular space, sphingolipids can interact with various signaling molecules, receptors, and enzymes, modulating diverse cellular processes, including proliferation, differentiation, apoptosis, inflammation, and metabolism (29). Dysregulation of sphingolipid metabolism has been associated with a variety of diseases, including neurodegeneration, cardiovascular disease, and other metabolic disorders (21, 29).

1.2.2 Exploring the mechanisms of ceramide-induced lipotoxicity in cells

Despite their involvement in numerous biological pathways, very little mechanistic insight has been gained into the metabolic function of sphingolipids as signaling molecules. Given these limited available resources, I have chosen to focus specifically on ceramide-mediated lipotoxicity in this thesis. Ceramide is the most well-studied species within the sphingolipid family, and therefore provides a promising avenue for investigating the physiological role of sphingolipids in inflammation and apoptosis (30).

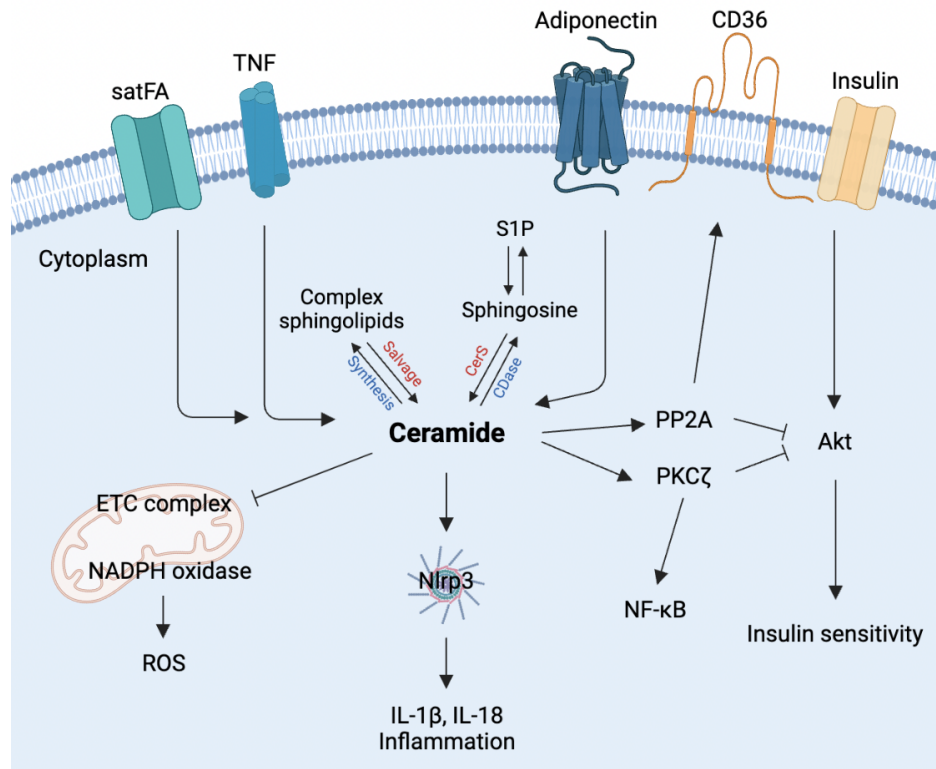


Figure 5. Ceramide-dependent lipotoxicity

Ceramide is produced in response to a variety of cellular stresses, such as TNF- α , and excessive free fatty acids (**Figure 5**). When ceramide accumulates within cells, it can activate

multiple stress signalling pathways, leading to the activation of pro-inflammatory kinases and their downstream targets (21, 30). In particular, ceramide accumulation activates the PP2A enzyme by disturbing its regulatory subunit, which, in turn, inhibits Akt kinase activity (**Figure 5**). Given that Akt kinase is a crucial mediator of insulin-stimulated responses, negative regulation by ceramide may contribute to insulin resistance (21, 25). Another signaling intermediates activated by ceramide accumulation is the PKC ζ , which is normally located in the cytoplasm of cells (**Figure 5**) (21, 31). When exposed to ceramide, PKC ζ is stimulated to translocate from the cytoplasm to the plasma membrane, where it becomes activated (21). Once activated, PKC ζ can regulate downstream signaling pathways that contribute to inflammation, including the inhibition of Akt activity and the activation of the transcription factor nuclear factor (NF- κ B) (21). Activated NF- κ B in the nucleus then induces the expression of various pro-inflammatory genes, such as COX-2 (21, 31). Additionally, ceramide promotes the secretion of pro-inflammatory cytokines, including IL-1 β and IL-18, by modulating the assembly of the NLRP3 inflammasome, a key regulator of innate immunity (21).

Excessive ceramide has also been associated with the impairment of mitochondrial respiratory chain activity, leading to enhanced generation of reactive oxygen species (ROS) and depletion of ATP (**Figure 5**) (32). According to the study by Zigdon *et al.*, C16 ceramide and sphingosine directly inhibited the activity of cytochrome c oxidase in CerS2 null mouse liver (33). This inhibition led to a state of chronic oxidative stress, ultimately resulting in apoptosis (33). These findings demonstrate the multifaceted role of ceramide in regulating inflammation, cellular fate, and their involvement in the development of metabolic disorders via lipotoxicity (32, 33).

1.2.3 Sphingolipids and metabolic disorders

Numerous studies have linked disruptions in sphingolipid homeostasis to the pathogenesis and progression of metabolic disorders, such as cardiovascular diseases (CVD), obesity, type 2 diabetes (T2D), and non-alcoholic fatty liver disease (NAFLD).

Cardiovascular diseases

Recent studies have identified plasma ceramide as an independent risk factor for CVD (34-36). Specifically, the elevated levels of ceramide and sphingomyelin in CVD patients were correlated with plaque instability and the severity of coronary artery stenosis (34). The study hypothesized that ceramide and sphingomyelin, carried by VLDL and LDL, promote lipoprotein infiltration into the vessel wall, contributing to endothelial dysfunction and atherosclerosis progression (34). Therefore, the ceramide score, calculated by combining various ceramide ratios, has been recently incorporated into the Cardiovascular Event Risk Test (CERT2) as a prognostic marker to identify residual inflammatory risk in CVD patients and to predict mortality (37).

Obesity and type 2 diabetes

Numerous studies have illuminated the pivotal role of sphingolipids in the physiological processes associated with insulin signaling and glucose homeostasis (21, 25, 30). The accumulation of sphingolipids, especially ceramides, has been extensively reported in insulin resistant tissues, such as skeletal muscle, liver, and adipose tissue, in both human and animal models with obesity and T2D (25). This finding corresponds to the notion presented in the

previous **chapter 1.2.2** that elevated ceramides disrupt the activity of Akt kinase, thereby inhibiting insulin signaling transduction (**Figure 5**).

Furthermore, ceramides have been implicated in the pathogenesis of pancreatic β -cell dysfunction in relation to T2D (25). Although further research is required to establish a causal relationship between ceramide accumulation and β -cell inflammation, recent studies suggest that ceramide accumulation in organelle membranes modulates their functions (38). Specifically, ceramide accumulation in the mitochondrial membrane can impair the electron transport chain, leading to a decrease in ATP production and ultimately lead to decreased insulin secretion and β -cell apoptosis (32, 38).

A study by Poss *et al.* suggests that ceramide score may serve as a promising clinical biomarker for predicting T2D remission (39). They found that ceramide levels decreased in patients with better insulin sensitization and diabetes resolution two years after gastric bypass surgery, suggesting that ceramide score could differentiate those who achieve sustained diabetes remission from those who will ultimately fail to maintain normal blood sugar levels (39). These findings provide valuable insight into the use of ceramide score as a diagnostic tool in clinics (39, 40).

Liver diseases

NAFLD is an umbrella term for a range of conditions characterized by a build-up of fat in the liver. Several studies have demonstrated that abnormal sphingolipid metabolism is a key physiologic cue in the pathogenesis of NAFLD (41-43). Indeed, changes in sphingolipid concentrations have shown a positive association with steatosis progression (42). Moreover, the accumulation of specific sphingolipids, notably C16 ceramide and sphingomyelinases, has been

linked to the second hit of NAFLD such as insulin resistance, inflammation, and cholesterol levels (42).

GSD Ia

Despite the abundance of studies examining triglycerides and cholesterol levels in GSD I patients, research investigating sphingolipid abnormalities in this population remains limited. A recent study by Hornemann *et al.* used a novel approach to study atypical sphingolipids in GSD Ia patients and suggested that these molecules have the potential to serve as new biomarkers for assessing metabolic control and the risk of peripheral neuropathy in GSD Ia (44). In particular, they found that GSD Ia patients had elevated levels of 1-deoxysphingolipids, which are known to be toxic to neurons and pancreatic β -cells (44, 45). Elevated levels of these atypical sphingolipids have also been frequently reported in studies on NAFLD and T2D, suggesting an intimate metabolic connection to carbohydrate and fatty acid metabolism (46, 47). Hence, we aimed to explore the sphingolipid profiles and their distinct alterations in GSD Ia more deeply.

1.3 Liquid chromatography coupled with tandem mass spectrometry

Liquid chromatography coupled with tandem mass spectrometry (LC-MS/MS) is an analytical technique widely used to identify and quantify biomolecules in laboratories today. This method involves two core components: 1) liquid chromatography, which allows separation of the molecules in a liquid sample, and 2) tandem mass spectrometry, which provides precise and specific molecular analysis by employing multiple mass analyzers (48, 49). The combination of these two components results in a highly sensitive and accurate analytical technique capable of detecting compounds even at extremely low concentrations in biological samples (50-52).

The targeted LC-MS/MS method is particularly advantageous in lipid studies as it allows for the simultaneous quantification of specific groups of metabolites in a single sample with high sensitivity and specificity (53). In contrast, untargeted screening methods produce information-rich and high-dimensional datasets containing numerous metabolites that are not predetermined (53). Thus, this screening modes are frequently utilized for a discovery approach, allowing for the identification of new biomarkers or pathways in clinical and forensic toxicology research (54). Given those reasons, we employed targeted LC-MS/MS method to accurately quantify a specific set of our target analytes – sphingolipids, and therefore to evaluate their role in the pathogenesis of GSD Ia.

1.3.1 Liquid Chromatography (LC)

LC separates molecules by exploiting the differential interactions between the analytes, the stationary phase, and the mobile phase, resulting in distinct migration rates of each analyte through the LC column and enabling their separation (49). Various types of LC are available depending on the physicochemical properties of the stationary and mobile phases (25). In our study, we have focused on the separation of non-polar and weakly polar lipids, and therefore have employed reversed-phase LC. In reversed-phase LC, the stationary phase consists of a non-polar hydrophobic material, while the mobile phase typically consists of a gradient of decreased polarity solvent mix, to enable gradual elution of non-polar species (**Figure 6**) (52).

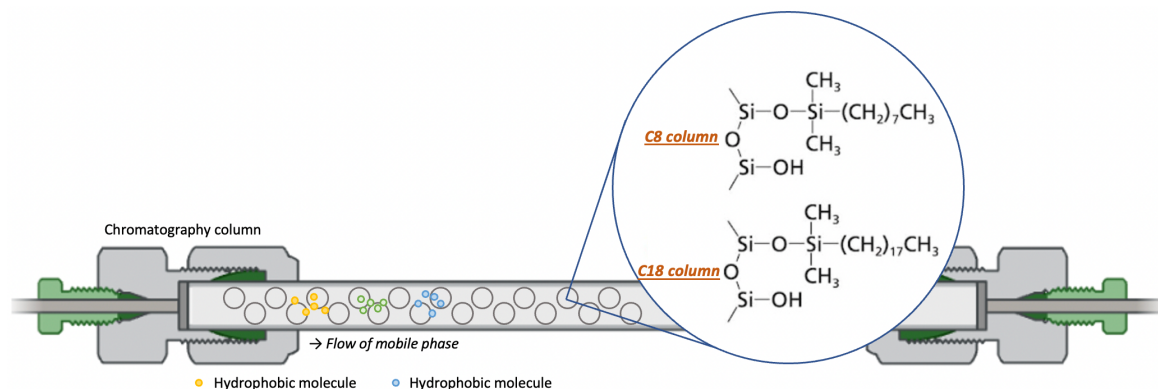


Figure 6. Reversed-phase chromatography elution

A sample solution containing target analytes is pumped through a stationary phase (LC column) by a mobile phase flowing through at high-pressure (49). The mobile phase's composition plays a critical role in the separation process by controlling the interactions taking place between sample components and the adsorbent (49). In reverse phase LC, separations are based on the chain length and degree of saturation of the sphingoid base and N-acyl fatty acid (**Figure 6**). The column is a thin-layer silica gel coated with hydrocarbons (55). Analytes initially interact with the hydrophobic stationary phase and are subsequently eluted with different retention times depending on the strength of their interaction with the stationary phase (52). Less polar compounds tend to interact more strongly with the stationary phase and, consequently, are eluted later (**Figure 6**). This unique retention time of each analyte can serve as a signature for identifying compounds. Once separated from the LC column, the compounds are detected and quantified by the MS/MS detector.

1.3.2 Tandem Mass Spectrometry (MS/MS)

As the name suggests, MS/MS performs mass analysis twice in succession to enhance sample identification and increase the accuracy of quantification. Targeted sphingolipidomics by MS/MS is commonly performed using triple quadrupole mass spectrometers in which the first and third quadrupoles are operated as mass analyzers and the second quadrupole proceeds with the fragmentation of the analytes via collision with Argon gas (**Figure 7**) (52). MS/MS offers several scanning modes, each with its own strengths and limitations. The choice of scanning mode depends on the specific research question and the properties of the analytes of interest. For the purposes of this study, we employed ‘Multiple Reaction Monitoring (MRM)’ technique, a highly sensitive method that enables the targeted detection of our analytes of interest (51). MRM mode achieves this by selectively screening the predefined precursor-to-fragment ion transitions, resulting in a specific analytical measurement (**Figure 8**).

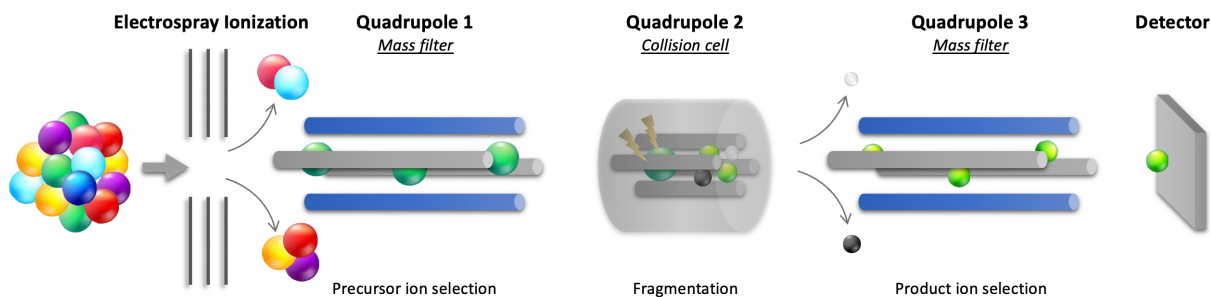


Figure 7. Scheme of tandem mass spectrometry (MS/MS)

The initiation of this technique is electrospray ionization (ESI), where the molecules are dispersed into highly charged droplets via a dispensing steel needle (52). As mass spectrometry measures the mass of charged particles, only electrically charged ions will be detected by the instrument. ESI provides several advantages for lipid analysis (56). Firstly, it has the capability

to ionize a broad range of lipids, including both polar and nonpolar species (52, 57, 58). Secondly, ESI is classified as a soft ionization technique, which produces ions with minimal fragmentation or rearrangement of the molecular structure (57). This characteristic is advantageous for the analysis of fragile lipids that are prone to fragmentation. Additionally, ESI is highly sensitive, enabling the detection of low-abundance lipids in complex mixtures (49, 52). This sensitivity is particularly useful in sphingolipidomics, where the identification and quantification of lipid species can be challenging due to their minor abundance in the lipid milieu of most mammalian cells.

The voltage is an adjustable parameter that controls the amount of energy applied to the sample cone of the ion source (59). This voltage parameter has a crucial role in the ionization process as it influences the fragmentation patterns of the analyte ions and the overall sensitivity of the analysis (59). Therefore, optimizing the cone voltage is fundamental to achieving the most optimal specificity of the LC-MS/MS method for the target analytes.

After the ionization, the ionized molecules are introduced to the first mass spectrometer (Q1) under a high vacuum (**Figure 7**) (52). The Q1 mass analyzer scans over a mass range to select a specific precursor ion (m/z) (48). Only ions with a selected m/z value are able to pass along the rods. Ions with other m/z values will have an unstable trajectory and consequently be expelled radially from the analyzer (48). At the collision cell (Q2), the selected m/z particles are intentionally fragmented into smaller parts by collision-induced dissociation with an inert argon gas (**Figure 7**) (48). As it affects the fragmentation of the precursor ion and the resulting product ions, selecting appropriate collision energy is essential in developing sensitive LC-MS/MS for targeted analytes (59, 60).

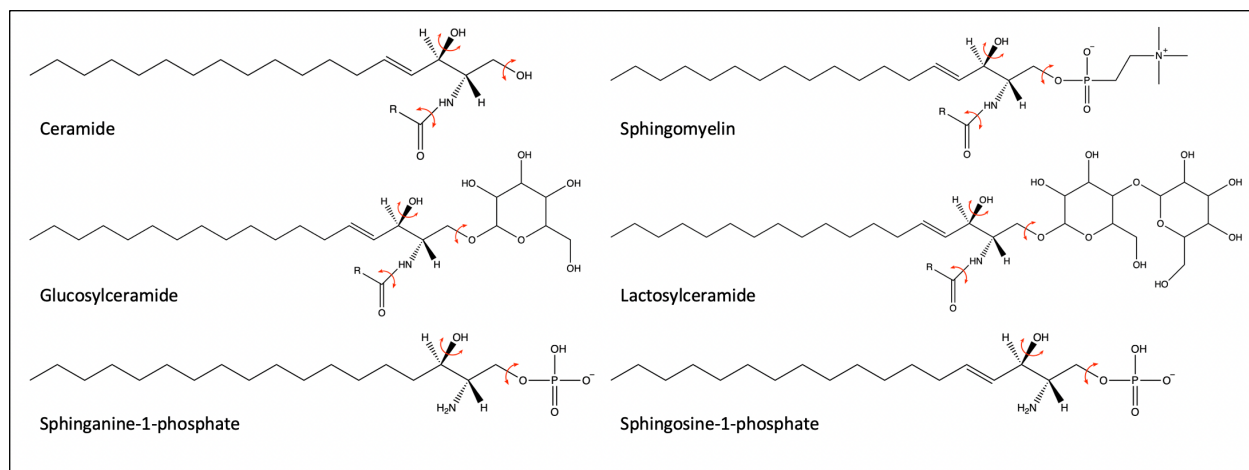


Figure 8. Typical MS/MS fragmentation patterns of sphingolipids: ceramide, sphingomyelin, glucosylceramide, lactosylceramide, sphinganine-1-phosphate and sphingosine-1-phosphate. The red arrows indicate the specific dissociation of molecular bonds within the structures of the analyzed compounds.

The resulting product ions are subsequently scanned in the third quadrupole (Q3), and only the ion with a specific predefined m/z value will be able to pass through the rods and reach the detector (**Figure 7**) (48). This transition of ions from the precursor to the product ion is called an ‘MRM transition’ (**Figure 8**). The transition is highly specific to the structural characteristics of the compound of interest and thus provides a high level of selectivity in detecting and quantifying the analyte (48).

1.4 Objective of the study

Dr. Mitchell's lab has established targeted LC-MS/MS methods to conduct qualitative and quantitative analysis of sphingolipids from diverse biological samples. Since sphingolipid metabolites are tightly interconnected with each other, it is necessary to investigate the multiple subfamilies simultaneously rather than a single metabolite. This study successfully developed and validated methods for targeted sphingolipidomic analysis, covering 20 sphingolipid species across various subgroups such as ceramide (Cer), sphingomyelin (SM), hexosylceramide (HexCer), lactosylceramide (LacCer), sphinganine-1-phosphate (Sa1P) and sphingosine-1-phosphate (S1P) from biological samples (**Table S1**). The developed methods were successfully applied to determine the sphingolipid profiles of liver and plasma samples from GSD Ia mouse models and compared with those of the wild type.

1.4.1 Primary objective

The fundamental objective of this study is to determine if circulating sphingolipids in GSD Ia are associated with increased risk or susceptibility to the development of liver adenomas and potentially their transformation to liver carcinomas.

1.4.2 Specific study aims

To achieve the primary objective of this study, the following specific aims will be investigated:

- **Aim 1:** To develop and validate targeted sphingolipidomic methods for comprehensive analysis of various sphingolipid subgroups (ceramide, sphingomyelin, hexosylceramide, lactosylceramide, sphinganine-1-phosphate and sphingosine-1-phosphate) in different biological samples (plasma and liver tissue) using the liquid chromatography-tandem mass spectrometry.
- **Aim 2:** To quantify the concentration of different sphingolipids in plasma and liver tissue from the GSD Ia mouse models.
- **Aim 3:** To compare the sphingolipid profiles between GSD Ia and non-alcoholic fatty liver disease (NAFLD) mouse studies.

CHAPTER 2. METHODOLOGY

2.1 Materials and Methods

2.1.1 Materials

2.1.1.1 Standards and solvents

Sphingolipid standards were obtained from Avanti Polar Lipids (Alabaster, USA, **Figure S2**). All solvents and reagents including formic acid (LC-MS grade, catalog no. A11750), water (LC-MS grade, catalog no. W64), acetonitrile (LC-MS grade, catalog no. A69554), isopropanol (LC-MS grade, catalog no. A4614), methanol (LC-MS grade, catalog no. A4564) and chloroform (LC-MS grade, catalog no. C6071) were from Thermo Fisher Scientific (Waltham, USA). Acquity Premier Ultra-Performance Liquid Chromatography interfaced with a Xevo TQ-S micro-Triple Quadrupole Mass Spectrometer was purchased from Waters (Milford, USA).

2.1.1.2 Internal standards

Exogenous odd-chain lipids are used as internal standards: C17 ceramide (d18:1/17:0) for all ceramide and sphingomyelin species, C16 glucosylceramide (d18:1/17:0) for glucosyl and lactosylceramide subgroups, d17:0 sphinganine-1-phosphate for sphinganine-1-phosphate species, and d17:1 sphingosine-1-phosphate for sphingosine-1-phosphate species.

2.1.1.3 Preparation of standard solution

5 mg of standard species were dissolved in methanol and chloroform to obtain 0.5 - 1.25 mg/ml of stock solutions of each sphingolipid species. The stock solutions were stored at - 20 °C until analysis (**Table S2**). Working solutions were prepared by diluting the stock solution with methanol.

2.1.2 Biological samples

Mouse plasma and liver tissues from 2-week-old wild type and GSD Ia models were procured from Dr. Dwight Koeberl's research laboratory at Duke University. All animal procedures were approved by the Institutional Animal Care and Use Committee at Duke University, and biological samples were collected according to relevant guidelines and regulations (IACUC number: A027-20-01). The specific gender information for the mouse samples were unavailable. The samples were delivered in sealed bags directly to MUHC for sphingolipid analysis.

The GSD Ia mouse model used in this study was generated based on a paper by Lei *et al.* (61). The G6Pase gene comprises five exons, and to disrupt it, a targeting vector was constructed, replacing exon 3 with a neomycin cassette (61). As a result, the mutant mice exhibited deficient G6Pase enzyme activity in both liver and kidneys, along with a range of phenotypic features similar to those observed in GSD Ia human patients, including hypoglycemia, hyperlipidemia, hyperuricemia, and lactic acidemia (61).

Due to the non-uniform distribution of lipids within liver lobules (30), it is a necessary prerequisite to homogenize liver tissue samples when studying endogenous sphingolipid concentrations. In our study, we employed several strategies to ensure accurate measurements of

hepatic sphingolipid content and minimize potential variations caused by differences in lipid distribution between different liver lobes. Firstly, we collected tissue samples from the same lobe of each mouse in all experimental groups, which allowed for meaningful comparisons of sphingolipid concentrations. Secondly, we developed a robust homogenization protocol for liver tissues using an ultrasonicator to ensure thorough and consistent homogenization. These strategies helped to ensure the accuracy and reliability of our measurements and provided valuable insights into the sphingolipid metabolism in the liver.

The following steps were taken to homogenize the liver tissue samples: a 50 mg aliquot of frozen liver tissue was suspended in 300 μ l of 1M NaCl solution and homogenized using an ultrasonicator (Sonics & Materials, Inc., USA, 20 kHz) at 30 % amplitude for 5 x 6 sec alternating on and off while cooling in an iced beaker. The homogenate was centrifuged at 13,800 RCF for 10 min at 4 °C to sink all impurities. The supernatant was aliquoted into 50 μ l each and stored at -80 °C freezer until analysis.

2.2 Sphingolipid extraction

The diversity of sphingolipids' polarity can be attributed to their molecular structure. To achieve efficient extraction of these compounds, we employed two distinct extraction methods in our experimental approach, taking into consideration their polarities. Specifically, we utilized the liquid-liquid extraction method to extract non-polar sphingolipids such as Cer, SM, HexCer, and LacCer. On the other hand, for the extraction of polar sphingolipids like Sa1P and S1P, we applied the single-phase extraction method (**Table 5**). A comprehensive description of each extraction method is in **Chapter 3.1**.

2.3 Quality control

Each batch of samples analyzed by LC-MS/MS requires quality control (QC) samples to evaluate variance across the data throughout the sample preparation, data acquisition, and data analysis steps. In our lab, we prepared QC samples by mixing a small aliquot of each volunteer's plasma. The data from the replicate QC samples were used to assess the reproducibility of the samples prepared using the same method. During the LC-MS/MS analysis, two QC samples were always analyzed to monitor the variance of the analytical process. If the variance was deemed too high (greater than 25 %), the corresponding batch was removed from the analysis.

2.4 Carryover

The needle wash solvent was composed of isopropanol:methanol:acetonitrile (50:30:20, v:v) with 0.1 % formic acid. To clean the exterior of the sample needle between injections, a needle wash setting utilizing a flow-through-needle technique by Waters® was employed.

Two blank samples (containing methanol:chloroform, 9:1, v:v) were consecutively analyzed throughout the instrument's run between each biological sample to assess potential contamination and possible carryover. If high carryover or significant shifts in the LC retention time were detected, the run was halted, and the instrument was cleaned before resuming. To maintain good LC performance, the column was cleaned before and after the batch run as appropriate.

2.5 Method validation

After developing an analytical method, it is essential to conduct method validation to ensure that the developed method meets predefined acceptance criteria and generates reliable

results. The guidelines for analytical method validation vary depending on the study purpose or the research location. In our study, we followed the US-FDA guidelines for method validation, which involved validating the method for its linearity, precision, accuracy, recovery, and reproducibility (62).

2.5.1 Linearity

Method linearity was tested using a ten-point calibration curve. Calibration standards were prepared by serial dilution. A graph was plotted with nominal concentration versus measured concentration of calibrants and a linear regression model was used to evaluate the coefficients of determination (or R^2) on the calibrators.

2.5.2 Precision and accuracy

Limits of detection (LOD) and limits of quantification (LOQ) were calculated in each analyte to evaluate the precision and accuracy of the method. The LOD value was defined by the visual evaluation. The determination of precision and accuracy was established according to the paper from Frej, *et al.*, 2015 and Liang *et al.*, 2012 (63, 64). The inter- and intraday precision and accuracy were determined by analyzing three replicates on the same day (intraday) and over three different days (inter-day). The precision was evaluated by calculating the coefficient of variation (CV) of replicates for each analyte. The accuracy was evaluated by calculating the relative error (RE) of replicates. Following the FDA guidelines, the acceptance criteria for precision and accuracy were defined as $\leq 20\%$.

2.5.3 Recovery

In compliance with FDA guidelines, we determined the analyte recovery by preparing two sets of samples. Set 1 was prepared by spiking the standard mix (a known amount of the analyte) before the extraction, while set 2 was the post-extraction spiked sample. To calculate recovery, we employed the methods outlined in Matuszewski *et al.* (2003) and Basit *et al.* (2015) (50, 65), using the following equation: $[(\text{Concentration of set 1}/\text{Concentration of set 2}) * 100]$.

2.5.4 Reproducibility

The reproducibility of the extraction methods was tested using a QC sample. The QC sample was split into two aliquots which were extracted and analyzed independently under the same conditions. Then the reproducibility was measured by comparing the measured concentration of replicates.

2.6 Statistics

LC-MS/MS data were acquired by MassLynx software and quantified by TargetLynx software. The unadjusted Wilcoxon rank sum test was used to measure the statistical significance of the difference in sphingolipid levels between groups, and *p-value* was set at 0.05. Statistics were performed using R studio software 3.5.2. The graphs were created using GraphPad Prism 9.0, and figures were drawn using BioRender (<https://biorender.com/>), and ChemDraw 20.1.

CHAPTER 3. RESULTS 1 – METHOD DEVELOPMENT AND VALIDATION

LC-MS/MS has emerged as a popular tool in lipidomic analyses, as it allows for the simultaneous measurement of a wide range of sphingolipids with high sensitivity and specificity (66). Optimizing each aspect and parameter of LC-MS/MS is crucial for their practical implementation, such as simplifying the sample preparation process, enhancing sphingolipid coverage, and minimizing the required sample quantity. These improvements are particularly important in translational research, which often involves a large number of samples with limited volumes per sample (66). Therefore, it is recommended that researchers and laboratories carefully develop and validate the methods to ensure efficient and accurate analysis. This chapter describes the detailed results from our optimization procedures of extraction methods and LC-MS/MS parameters.

In this study, we succeeded in developing and validating a robust LC-MS/MS bioanalytical assay for sphingolipid quantification in biological samples. The following subgroups of sphingolipids were included: six ceramides (Cer), five sphingomyelins (SM), four hexosylceramides (HexCer), three lactosylceramides (LacCer), and two phosphate sphingolipids (Sa1P and S1P) (**Table S1**). As it was practically impossible to separate galactosylceramide and glucosylceramide using our current LC-column and technique, we employed glucosylceramide as a surrogate for the hexose-linked ceramides (HexCer) (67).

3.1 Sphingolipid extraction

Sphingolipids are a large family of lipids with a vast array of molecular structures, comprising of various species found in biological systems, according to lipidmaps.org. Their structural diversity provides them with distinct polarity characteristics (**Figure 9**).

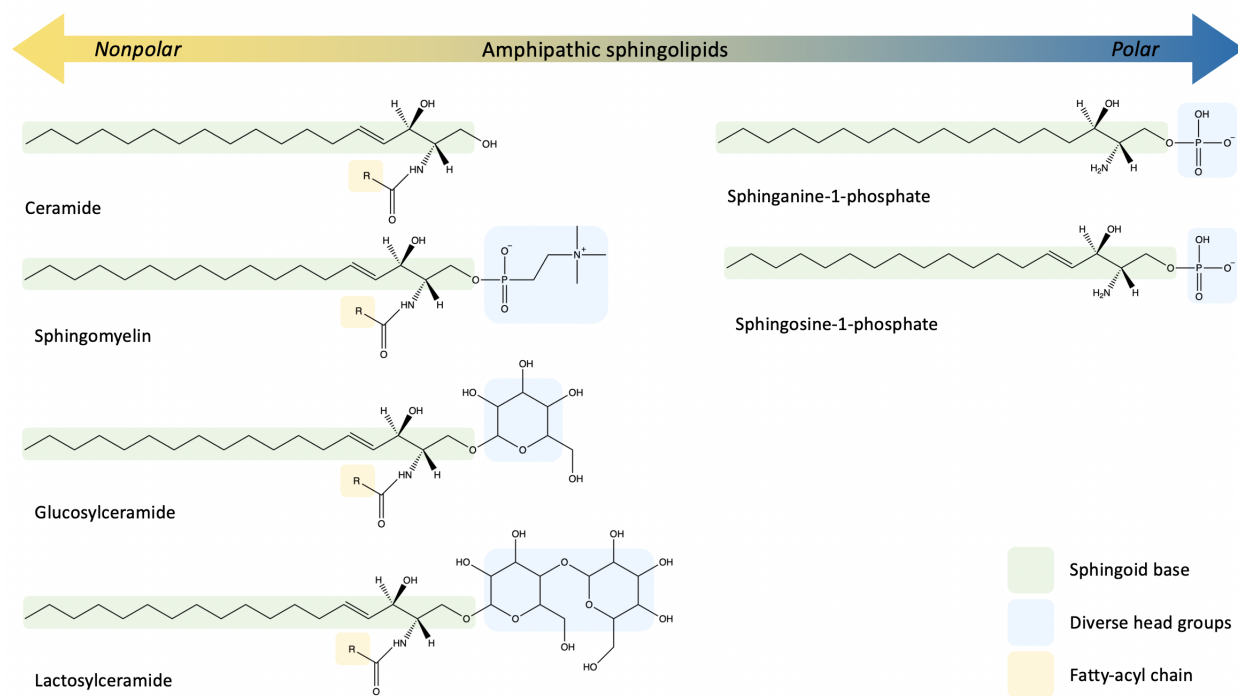


Figure 9. Amphipathic sphingolipids

The bidirectional arrow represents the polarity of molecules, with the right side indicating greater polarity and the left side indicating lower polarity. The structures of each sphingolipid are shown in three distinct regions. The green box area corresponds to the sphingoid base, which serves as the backbone of each molecule. The blue box area represents the head group, and the yellow box indicates the fatty-acyl chain.

Ceramide and complex sphingolipids consist of a sphingoid base that is N-acylated with a long fatty acid at the amino group in the C-2 position, while diverse head groups are present at the C-1 position for more complex sphingolipids (**Figure 9**). As a result of their long fatty acyl chain, a hydrophobic tail, our target ceramide and complex sphingolipids exhibited hydrophobic

characteristics, despite the presence of a hydrophilic head group. In contrast, phosphate sphingolipids possess a relatively simpler molecular structure: a sphingoid base with a phosphate head group at the C-1 position. Their polarity is thus influenced by the phosphate head group, rendering them more polar than other sphingolipid subgroups (**Figure 9**).

In our experimental approach, we adopted two distinct extraction methods, with careful consideration given to the polarities of the targeted compounds, to ensure efficient extraction (**Table 2**). Specifically, we utilized the liquid-liquid extraction method for more hydrophobic sphingolipids (ceramide and complex sphingolipids). Conversely, for the extraction of polar sphingolipids like Sa1P and S1P, we applied the single-phase extraction method.

	Ceramide and complex sphingolipids	Phosphate sphingolipids
Target analytes	Ceramide, Sphingomyelin, Hexosylceramide, Lactosylceramide	Sphinganine 1 phosphate, Sphingosine 1 phosphate
Extraction method	Liquid-liquid extraction	Single-phase extraction method
< LC conditions >		
LC column	CORTECS C8	CSH C18
Column temperature	40 °C	55 °C
Flow	0.3 ml/min	0.4 ml/min
Buffer A	acetonitrile:water (20:80, v:v), with 0.1 % formic acid	
Buffer B	acetonitrile:isopropanol (20:80, v:v), with 0.1 % formic acid	
Total run time	11 min	6.25 min

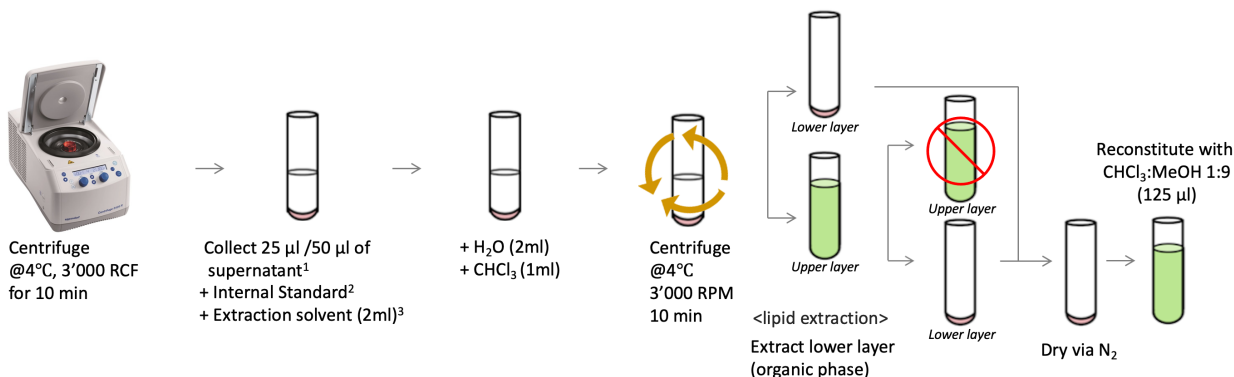
Table 2. Overview of extraction and LC methods according to the type of sphingolipids

3.1.1 Liquid-liquid extraction method

The liquid-liquid extraction method separates the complex compounds based on their relative solubilities in two different liquids: aqueous versus organic solvents (**Figure 10.A**). The extraction protocol was developed based on the ‘Bligh and Dyer’ method. Plasma and liver aliquot samples were transferred into a borosilicate tube. Samples were spiked with 25 µl of the

internal standard mix. 2 ml of an ice-cold chloroform:methanol (1:2, v/v) with 0.1 % TFA mixture was added and mixed for 30 seconds with a Vortex®. Then, liquid-liquid extraction was performed by adding 1 ml of chloroform and 2 ml of water sequentially. The samples were mixed with a Vortex® and centrifuged at 3,000 RPM, 4 °C for 10 min to separate the aqueous (upper) and organic (lower) phases. The lower organic phase was removed carefully with a Pasteur pipette, penetrating the interface, and was transferred into a separate test tube. The remainder were re-extracted as before with an additional 1 ml of chloroform. The collected organic phase was dried under nitrogen gas and reconstituted in 125 µl of a chloroform:methanol (1:9, v/v) mixture.

A. Liquid-liquid extraction method



B. Protein precipitation method

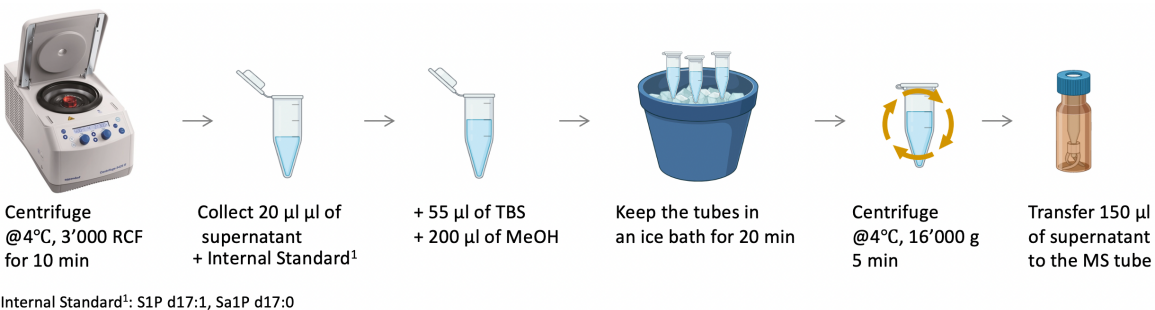


Figure 10. Illustration of sphingolipid extraction protocols

3.1.2 Single-phase extraction method

Single-phase extraction method presented by Frej *et al.* was primarily used to optimize our protocol for phosphate sphingolipids (**Figure 10.B**) (63). Plasma samples were defrosted and centrifuged at 3,000 RCF, 4 °C for 10 min. 20 µl of biological samples were transferred into a new microcentrifuge tube. Samples were spiked with 25 µl of the internal standard mix and mixed with a Vortex®. Then, 55 µl of TBS (50 mM Tris-HCl pH 7.5, 0.15 M NaCl) was added to the sample tube and mixed. Afterwards, the precipitation solvent (200 µl of methanol) was added and mixed with a Vortex® at maximum speed. The sample tubes were kept in an ice bath for 20 min. The tubes were centrifuged at 16,000 RCF, 4 °C for 5 min after which 150 µl of supernatant was transferred to an MS vial.

3.2 LC-MS/MS conditions

Liquid chromatography coupled with electrospray ionization tandem mass spectrometry (LC-MS/MS) was used to quantify sphingolipid concentrations in samples.

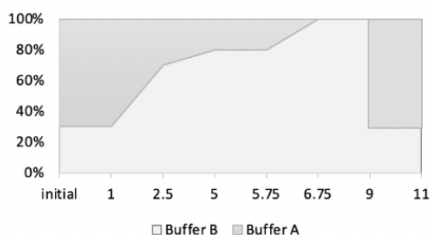
3.2.1 LC separation conditions

3.2.1.1 Ceramide and complex sphingolipids

Target analytes (Cer, SM, HexCer, and LacCer) were separated by a reverse-phase LC using ACQUITY UPLC CORTECS C8 column (90Å, 2.7 µm, 4.6 mm X 150 mm, Waters, MA, USA). Mobile phases A and B consisted of acetonitrile:water (20:80, v:v), with 0.1 % formic acid, and acetonitrile:isopropanol (20:80, v:v), with 0.1 % formic acid, respectively. The flow rate was 0.3 ml/min, and the column temperature was set at 40 °C (**Table 2**). The total run time was 11 min; the gradient of mobile phases A and B is shown in **Figure 11.A**. The injection

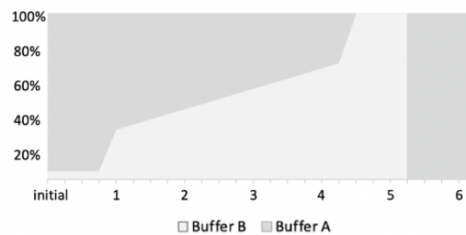
volume was 1 μ l. Typical MS conditions were a capillary voltage of 0.5 kV. The source temperature was set at 150 $^{\circ}$ C. Desolvation gas and cone gas (N_2) flow were set to 1,000 L/hr and 50 L/hr, respectively. **Figure S1.A-C** illustrates the separation of species achieved with various retention times.

A. CORTECS C8 column



Time (min)	Flow (ml/min)	Buffer A %	Buffer B %	Curve
1	initial	70.0	30.0	
2	1.00	70.0	30.0	6
3	2.50	30.0	70.0	6
4	5.00	20.0	80.0	6
5	5.75	20.0	80.0	6
6	6.75	0.0	100.0	6
7	9.00	0.0	100.0	1
8	11.00	70.0	30.0	1

B. CSH C18 column



Time (min)	Flow (ml/min)	Buffer A %	Buffer B %	Curve
1	initial	95.0	5.0	
2	0.75	95.0	5.0	6
3	1.00	70.0	30.0	6
4	4.25	30.0	70.0	6
5	5.25	0.0	100.0	1
6	6.25	100.0	0.0	1

Figure 11. The chromatographic gradient used for sphingolipid separation.

The detailed settings and gradient run for the UPLC are presented in **A.** for CORTECS C8 column and **B.** for CSH C18 column.

3.2.1.2 Phosphate sphingolipids

For phosphate sphingolipids (Sa1P and S1P), ACQUITY UPLC CSH C18 column (130 \AA , 1.7 μ m, 2.1 mm X 50 mm, Waters, MA, USA) was used. Mobile phases A and B consisted of acetonitrile:water (20:80, v:v), with 0.1 % formic acid, and acetonitrile:isopropanol (20:80, v:v), with 0.1 % formic acid. The flow rate of CSH C18 column was 0.4 ml/min and the column temperature was set at 55 $^{\circ}$ C (**Table 2**). The injection volume was 1 μ l and the total run time was 6.25 min. The gradient of mobile phases is shown in **Figure 11.B**. The standard MS conditions for phosphate sphingolipid analysis were a capillary voltage of 0.5 kV, with the

source temperature set at 500 °C. Desolvation gas and cone gas (N₂) flow were set to 1,000 L/hr and 50 L/hr, respectively. **Figure 12** shows the separation of phosphate species achieved with different retention times.

3.2.2 IntelliStart™

Waters® provides IntelliStart™ software / interface which automatically calibrates the instrument, tunes the mass spectrometry, and develops MRM methods for each analyte. All parameters including the optimized cone voltages, collision energies, and precursors and product ions for analytes were obtained using the IntelliStart™. For the analysis of Cer, SM, HexCer, and LacCer, the mass spectrometry was operated in the positive ionization mode.

The phosphate head group of the phosphate sphingolipids allows for both positive and negative ionization modes to be used in mass spectrometry for their detection. Hence, we employed both ionization modes of MRM mass spectra to quantify Sa1P and S1P in QC samples, which were acquired from a single LC-MS/MS analysis. The combined use of two ionization modes provided high sensitivity and specificity, enabling accurate detection and quantification of the analytes. The complete panel of MRM transitions and optimized parameter settings are described in **Table 3**.

Compound	Mode	MRM transitions		Cone Voltage (eV)	Collision Energy (eV)	RT (min)
		Precursor ion <i>m/z</i>	Product ion <i>m/z</i>			
Ceramide						
C14 Cer d18:1 14:0	ESI+	510.45	264.33	46	26	3.8
C16 Cer d18:1 16:0	ESI+	538.42	264.34	46	28	4.1
C20 Cer d18:1 20:0	ESI+	594.48	264.26	68	26	4.7
C22 Cer d18:1 22:0	ESI+	622.51	264.33	22	26	5.0
C24 Cer d18:1 24:0	ESI+	650.61	264.33	64	32	5.4
C24:1 Cer d18:1 24:1	ESI+	648.59	264.33	48	26	5.0
Sphingomyelin						
C16 SM d18:1 16:0	ESI+	703.54	184.03	16	30	3.8
C16:1 SM d18:1 16:1	ESI+	701.46	124.97	12	72	3.6
C18 SM d18:1 18:0	ESI+	731.57	184.03	10	28	4.0
C24 SM d18:1 24:0	ESI+	815.53	184.09	10	30	5.0
C24:1 SM d18:1 24:1	ESI+	813.58	184.03	10	34	4.7
Hexosylceramide						
C16 HexCer d18:1 16:0	ESI+	700.73	264.27	22	32	3.9
C18 HexCer d18:1 18:0	ESI+	727.48	264.58	8	30	3.9
C18:1 HexCer d18:1 18:1	ESI+	726.48	264.32	18	40	3.9
C24:1 HexCer d18:1 24:0	ESI+	810.58	264.27	4	46	4.6
Lactosylceramide						
C16 LacCer d18:1 16:0	ESI+	862.78	264.26	2	36	3.7
C18 LacCer d18:1 18:0	ESI+	890.55	264.26	16	40	4.0
C24 LacCer d18:1 24:0	ESI+	974.65	264.33	2	52	4.8
phosphate sphingolipids						
Sa1P d18:0	ESI+	382.23	284.28	72	12	3.3
	ESI-	380.17	78.84	42	28	3.3
S1P d18:1	ESI+	380.22	264.25	6	14	3.1
	ESI-	378.15	78.84	42	24	3.1

Table 3. MRM transitions and optimized parameters for each analyte.

MRM transitions, cone voltage, collision energy, and retention time for 20 target analytes are presented.

3.3 Method validation

3.3.1 Ceramide and complex sphingolipids

Linearity was analyzed using the calibration curve at 10 points, which showed excellent correlation coefficients (R^2) ranging from 0.991 to 0.999, indicating a strong linear relationship (**Table 4**). Reproducibility of ceramide and complex sphingolipid species was above 88.1 %. Recovery of sphingolipid species was between 87.7 % and 112.6 %. The intra and inter-day precision (CV) was within the range of 2.8 % – 18.8 %. The intra and inter-day accuracy (RE) was between 3.2 % and 15.5 %. LOQ and LOD of each species are presented in the **Table 4**.

3.3.2 Phosphate sphingolipids

To evaluate linearity, we used the calibration curve at 10 concentration levels, and observed correlation coefficients (R^2) ranging from 0.996 to 0.997. These results indicated a strong linear relationship between the instrumental measurements and nominal concentrations. (**Table 4**). The results of recovery and reproducibility showed 90.5 – 98.2 % and 106.2 – 112.6 % respectively. In terms of precision and accuracy, we analyzed three replicates at three concentration levels. The intraday precision (CV) of the phosphate sphingolipids ranged from 1.5 % to 3.5 %, with an accuracy (RE) of 7.5 % to 10.8 %. The inter-day precision was within 1.7 % to 5.6 %, with an accuracy of 10.4 % to 13.0 %. LOQ and LOD of phosphate sphingolipids are displayed in the **Table 4**.

Sphingolipid	Linearity (R ²)	Rep. (%)	Recovery (%)	Precision (% CV)				Accuracy (% RE)				LoQ (nM)	LoD (nM)
				Intra-day (n=3)		Inter-day (n=3)		Intra-day (n=3)		Inter-day (n=3)			
				Mean	SD	Mean	SD	Mean	SD	Mean	SD		
Ceramide													
C14 Cer d18:1 14:0	0.9993	95.2	95.7	2.9	0.6	8.2	7.5	9.7	6.3	7.7	5.0	10.0	1.3
C16 Cer d18:1 16:0	0.9996	94.2	100.8	4.8	0.4	5.6	2.8	4.7	1.1	5.4	3.2	11.8	1.5
C20 Cer d18:1 20:0	0.9992	93.0	108.8	8.7	8.7	13.0	17.4	9.8	9.6	8.5	11.0	10.7	1.3
C22 Cer d18:1 22:0	0.9993	96.8	111.0	10.8	2.7	7.2	5.3	9.7	2.1	10.4	1.9	10.2	1.3
C24 Cer d18:1 24:0	0.9999	96.5	104.2	9.3	12.0	7.4	5.4	8.7	8.9	5.8	5.1	39.1	4.9
C24:1 Cer d18:1 24:1	0.9999	97.3	104.5	5.6	2.1	8.1	5.8	5.3	3.2	6.9	2.3	19.6	2.5
Sphingomyelin													
C16 SM d18:1 16:0	1	99.1	98.4	4.0	2.3	3.8	2.7	3.3	1.1	4.1	3.3	45.2	2.9
C16:1 SM d18:1 16:1	0.9999	100.0	93.7	4.4	1.4	4.7	4.3	3.4	1.0	5.1	2.5	31.9	2.0
C18 SM d18:1 18:0	1	90.7	93.6	3.1	1.8	3.3	3.2	3.2	1.4	5.8	6.0	46.6	3.0
C24 SM d18:1 24:0	0.9999	95.6	108.7	7.8	8.1	7.3	2.6	6.3	6.6	5.7	2.2	78.0	5.0
C24:1 SM d18:1 24:1	1	98.4	112.4	2.8	1.3	7.8	7.5	3.2	1.5	6.2	6.4	21.5	2.8
Glucosyl/Lacosylceramide													
C16 GlcCer d18:1 16:0	0.9986	89.5	93.7	3.7	0.5	4.8	4.0	5.1	1.1	3.7	3.0	10.9	1.4
C18 GlcCer d18:1 18:0	0.9976	93.3	87.7	10.3	6.1	15.1	11.0	8.8	3.4	11.5	6.1	10.5	1.3
C18:1 GlcCer d18:1 18:1	0.9999	97.5	96.7	9.4	11.2	3.1	1.2	6.8	6.6	3.8	2.0	10.6	1.3
C24:1 GlcCer d18:1 24:1	0.9991	99.9	105.3	11.0	3.2	7.5	3.3	8.7	3.0	6.4	3.3	9.4	1.2
C16 LacCer d18:1 16:0	0.9989	96.1	90.8	10.8	12.1	8.6	10.8	10.1	5.6	9.2	6.7	12.9	1.6
C18 LacCer d18:1 18:0	0.9911	88.1	108.4	16.3	3.7	18.8	13.2	15.5	4.4	18.4	13.9	10.3	2.6
C24 LacCer d18:1 24:0	0.9993	96.8	93.1	15.1	20.9	8.5	9.7	10.7	12.3	8.2	7.8	11.7	1.5
Sphingolipid-1-phosphate													
Sa1P d18:0 (ES +)	0.9964	91.0	111.0	3.5	4.0	5.6	3.4	7.5	10.5	13.0	6.9	27.0	0.9
Sa1P d18:0 (ES -)	0.9964	98.2	112.6	2.3	1.0	2.7	1.6	10.8	9.8	12.9	7.0	27.0	0.9
S1P d18:1 (ES +)	0.9964	90.5	109.1	1.5	1.7	1.7	1.3	10.4	9.1	11.2	7.1	27.0	0.9

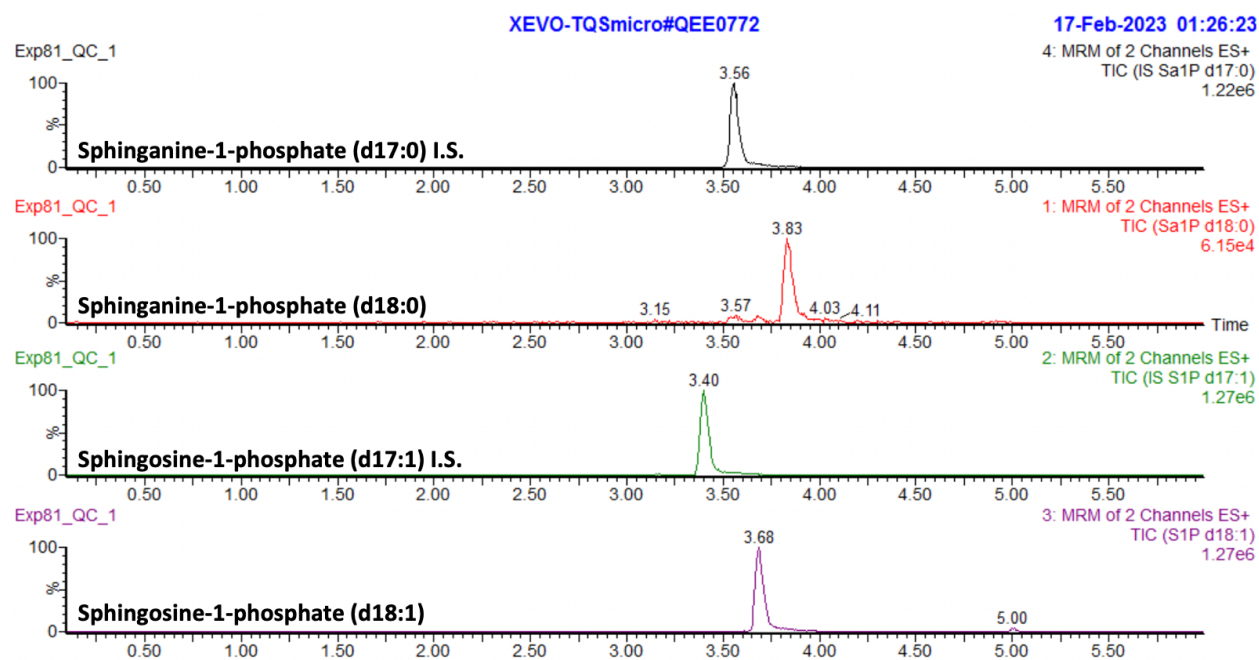
S1P d18:1 (ES -)	0.997	92.2	106.2	2.0	2.7	3.7	1.2	9.8	9.9	10.4	5.9	27.0	0.9
------------------	-------	------	-------	-----	-----	-----	-----	-----	-----	------	-----	------	-----

Table 4. Validation parameters in LC-MS/MS: linearity, reproducibility (Rep.), recovery, intra- and inter-day precision, intra- and inter-day accuracy, LOQ and LOD

3.4 Quantification of sphingolipids in QC samples

The developed liquid-liquid extraction methods were utilized in the analysis of the GSD Ia mice project. The pertinent findings will be presented in the upcoming chapter. Unfortunately, due to constraints in sample availability and the project timeline, the results of single-phase extraction method for phosphate sphingolipids could not be included. To address this limitation, the results of phosphate sphingolipids from QC samples have been incorporated.

A. ESI + mode



B. ESI – mode

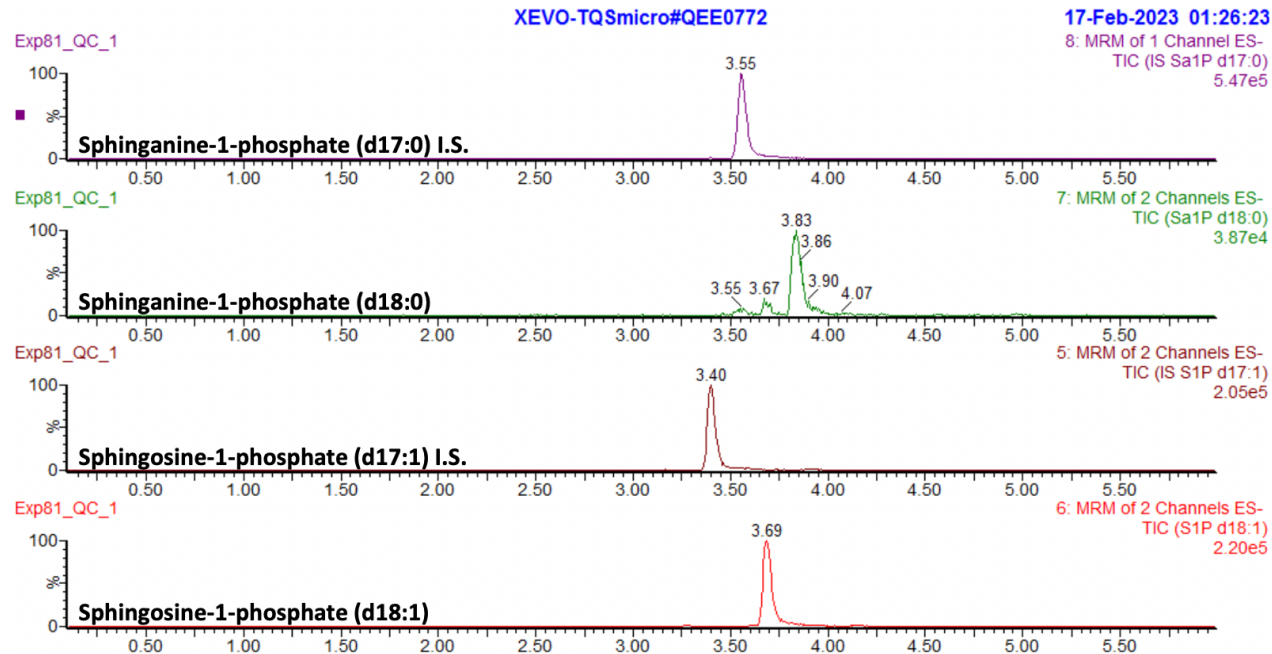


Figure 12. The chromatographic separation of phosphate sphingolipids from extracted QC sample

A. The chromatographic separation of phosphate sphingolipids was obtained under positive ion mode (ESI +). **B.** The chromatographic separation presented was obtained under negative ion mode (ESI –). IS: Internal standard, TIC: Total ion chromatogram

Due to the similar molecular structures of Sa1P and S1P, achieving separation with distinct retention times has been challenging. This challenge is further complicated in biological samples due to the interference caused by components in the sample matrix (50, 59). After attempting various combinations of mobile phases and gradient ratios, we were able to determine the optimized LC conditions that effectively separated each phosphate sphingolipid species with different retention times (**Figure 12**).

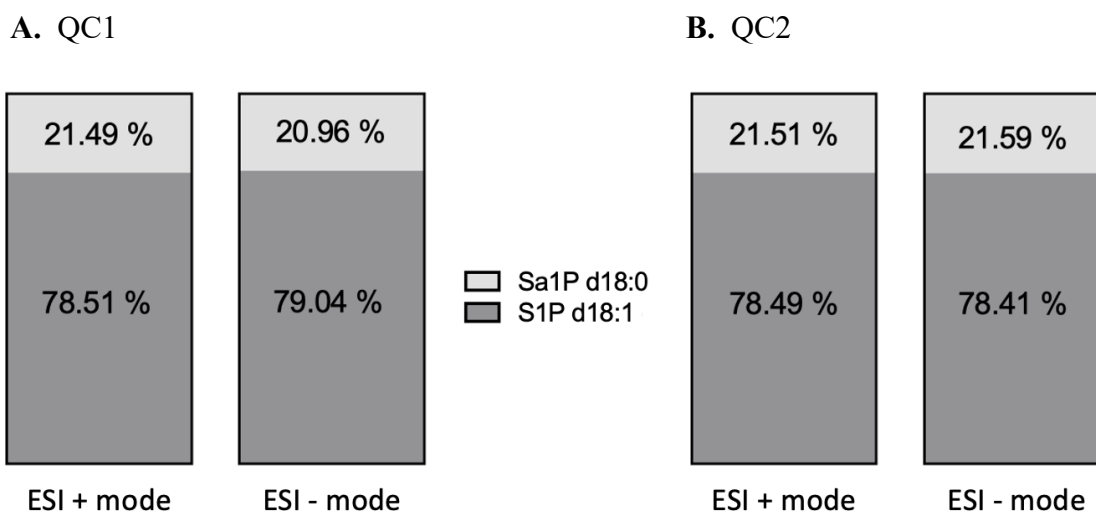


Figure 13. The measured concentration of phosphate sphingolipids in QC samples using single-phase extraction and targeted sphingolipidomic methods.

A. and **B.** show the levels of phosphate sphingolipids in QC samples analyzed independently. The light grey bars represent Sa1P levels, while the dark grey bars represent S1P levels.

Figure 13 shows the measured concentrations of phosphate sphingolipids (Sa1P and S1P) in QC samples comprising a mixture of human plasma. Notably, both ionization mode, ESI + and ESI – showed comparable results for quantification of Sa1P and S1P in QC samples.

Figure 13.A and **13.B** present the data from individual batches of phosphate sphingolipid experiments. Comparison of the two results indicates that the methods of single-phase extraction are highly reproducible and accurate, as demonstrated in the previous **Chapter 3.2.2**. Additional studies are still required to establish the statistical equivalence of quantitative results of phosphate sphingolipids across both ionization modes.

CHAPTER 4. RESULTS 2 – TARGETED SPHINGOLIPIDOMICS in GSD Ia MICE

This chapter presents a comparative analysis of the sphingolipid profiles obtained from the liver and plasma samples of both wild type and GSD Ia mouse models. Specifically, the results include 18 different sphingolipid species from 4 subgroups including ceramide, sphingomyelin, hexosylceramide, and lactosylceramide (**Figure S1**).

4.1 Elevated sphingolipid levels in GSD Ia mice plasma

In this study, a *G6Pase* knockout mouse was utilized as a GSD Ia mouse model, representing the pathophysiology observed in human GSD Ia patients. Plasma sphingolipids were quantified from both the GSD Ia (n = 5) and the wild type (n = 5) groups.

14 detected sphingolipid species exhibited a significant increase in the GSD Ia group ($p < .025$, **Table 5**). Major elevation was observed in ceramide: 106.0-fold for C16 Cer, 40.2-fold for C20 Cer, 24.8-fold for C22 Cer, 31.7-fold for C24 Cer, and 28.8-fold for C24:1 Cer.

The levels of hexosylceramide and lactosylceramide were measured to observe the complex sphingolipid metabolism in GSD Ia mice. All hexosylceramide and lactosylceramide were significantly increased in the plasma of GSD Ia mice. In particular, C24 LacCer showed a huge increase of 39.5-fold compared to other complex sphingolipid species.

Concentration (nM)														
	Cer					LacCer		HexCer			SM			
	C16	C20	C22	C24	C24:1	C16	C24	C16	C18	C24:1	C16	C18	C24	C24:1
WT	79.7	23.9	257.6	984.9	738.9	173.2	14.7	948.0	294.6	1548.3	16486.0	4868.6	4921.9	17791.9
GSD Ia	8441.4	960.86	6389.7	31176.3	21300.7	1268.5	579.8	17291.0	10627.2	50906.6	28217.7	12074.8	42321.3	93034.6
fold	106.0	40.2	24.8	31.7	28.8	7.3	39.5	18.2	36.1	32.9	1.7	2.5	8.6	5.2
<i>p-value</i>	<.025	<.025	<.025	<.025	<.025	<.025	<.025	<.025	<.025	<.025	<.025	<.025	<.025	<.025

Table 5. The comparison of sphingolipid concentrations in mouse plasma

The fold change was calculated as the concentration of each species in GSD Ia mice divided by the concentration of the same species in wild type mice. **Blue numbers** indicate higher sphingolipid concentrations in GSD Ia mice compared to wild type mice. Statistically significant numbers are shown in bold in the fold row.

Concentration (mol/g)																	
	Cer						LacCer			HexCer			SM				
	C14	C16	C20	C22	C24	C24:1	C16	C18	C24	C16	C18:1	C24:1	C16	C16:1	C18	C24	C24:1
WT	1.7E-10	6.7E-09	2.0E-09	2.4E-08	5.1E-08	4.5E-08	9.3E-10	4.1E-11	1.7E-09	1.0E-08	9.4E-12	5.9E-08	3.8E-08	5.4E-09	9.7E-09	9.0E-08	1.1E-07
GSD Ia	1.0E-10	7.8E-09	2.6E-09	2.3E-08	2.5E-08	3.4E-08	1.8E-09	6.8E-11	1.3E-09	1.1E-08	4.5E-12	3.2E-08	3.1E-08	3.6E-09	9.1E-09	3.3E-08	5.1E-08
fold	0.6	1.2	1.3	0.9	0.5	0.8	2.0	1.6	0.8	1.1	0.5	0.5	0.8	0.7	0.9	0.4	0.5
<i>p-value</i>	<.025	0.42	<.05	0.55	<.025	<.025	<.025	0.10	0.10	0.68	0.10	<.025	<.025	<.025	1	<.025	<.025

Table 6. The comparison of sphingolipid concentrations in mouse liver tissue

The fold change was calculated as the concentration of each species in GSD Ia mice divided by the concentration of the same species in wild type mice. **Blue numbers** indicate higher sphingolipid concentrations in GSD Ia mice compared to wild type mice, while **red** indicates lower concentrations. Statistically significant numbers are shown in bold in the fold row.

The data presented in **Table 5** demonstrate a significant increase in plasma levels of all sphingomyelins in GSD Ia mice. Notably, the degree of elevation observed in sphingomyelins was relatively smaller than that observed in other species. Specifically, the increase was 1.7-fold for C16 SM, 2.5-fold for C18 SM, 8.6-fold for C24 SM, and 5.2-fold for C24:1 SM. Despite the diverse degrees of increase for each species and subgroup, all sphingolipid species were observed to be significantly elevated in the GSD Ia mouse models.

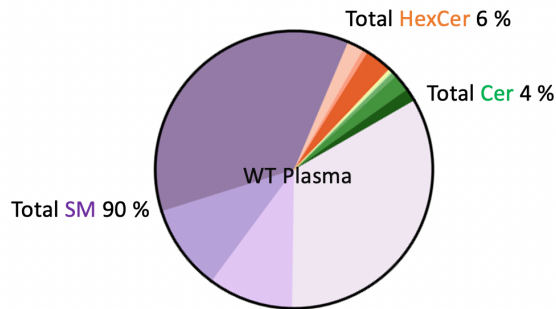
4.2 Hepatic sphingolipid metabolism in GSD Ia mice

To gain insight into the disruption of hepatic sphingolipid metabolism, we examined the individual species from 4 different sphingolipid classes in liver tissues obtained from 2-week-old mice. The liver tissue samples were collected from the same lobe of each mouse to compare sphingolipid concentrations between the different groups of mice (68). **Table 6** provides a summary of the sphingolipid alterations detected in GSD Ia liver tissues compared to those of the wild type. Out of the 17 sphingolipid species, 10 exhibited statistically significant changes in the GSD Ia mice. Interestingly, the pattern of perturbations in liver tissue differed from that observed in the plasma data. Depending on the acyl chain length of the sphingolipids, the fluctuation patterns varied, with an increase in the long-chain Cer, C16 Cer and C20 Cer, and a decrease in very-long-chain Cer, C24 Cer and C24:1 Cer. All sphingomyelin species showed decreased levels in the GSD Ia mice: 0.8-fold in C16 SM, 0.7-fold in C16:1 SM, 0.4-fold in C24 SM and 0.5-fold in 24:1 SM.

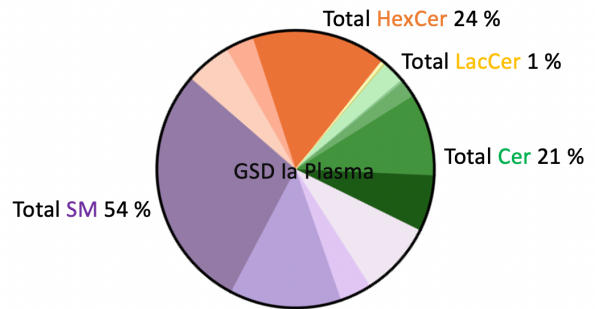
4.3 Disturbed sphingolipid profiles in GSD Ia mouse plasma and liver

In this study, we aimed to establish the distinct molecular profiles of sphingolipid classes in GSD Ia mice. To achieve this, we utilized pie charts to visually represent the relative abundance of each sphingolipid class within wild type and GSD Ia groups (**Figure 14**). These pie chart revealed clear disruptions in the distributions of sphingolipid subgroups in GSD Ia.

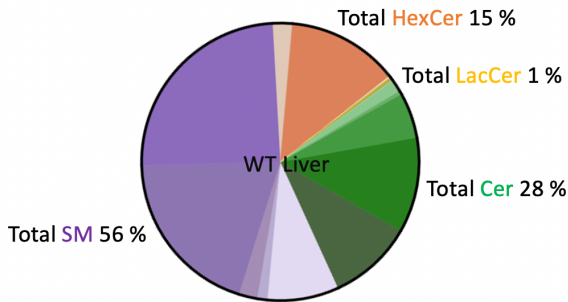
A.1. WT Mouse Plasma



A.2. GSD Ia Mouse Plasma



B.1. WT Mouse Liver



B.2. GSD Ia Mouse Liver

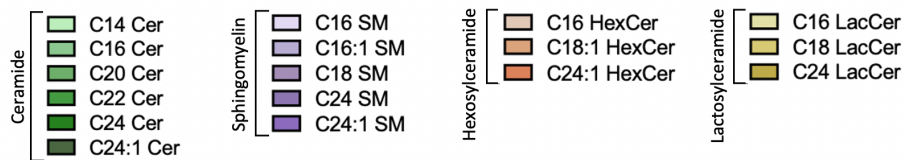
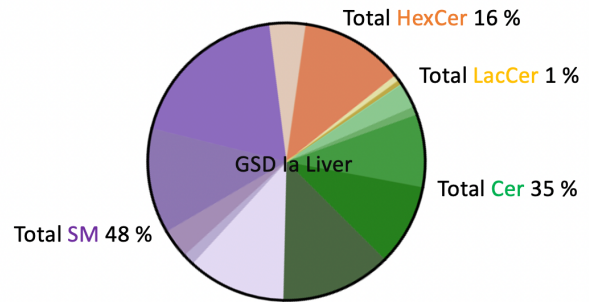


Figure 14. Compositional analysis representing the abundance of sphingolipids in A. mouse plasma and B. Mouse liver tissue.

In WT mouse plasma, sphingomyelins were found to be predominant, accounting for 90 % of total sphingolipids, with 44.1 % of long-chain SM (C16 – C18 SM) and 45.9 % of very-long-chain SM (C24 – C24:1 SM) (**Figure 14A.1**). Hexosylceramides followed sphingomyelins with 6%, and ceramides with 4% was the next most abundant species. Although the absolute levels of each sphingolipid species were significantly increased in GSD Ia mice (**Table 5**), the composition of individual subgroups changed in diverse patterns. Specifically, in GSD Ia mouse plasma, the proportion of sphingomyelins significantly decreased from 90 % to 54 %, while the proportion of hexosylceramides and ceramides increased up to 5-fold. Intriguingly, the composition of sphingomyelins was also altered in GSD Ia mice, with long-chain SM making up for only 23 % of total sphingomyelins, while very-long-chain SM made up 77 % of total sphingomyelin content (**Figure 14A.2**).

Figure 14B displays the sphingolipid profiles of liver tissue from wild type and GSD Ia mice samples. In wild type mouse liver, sphingomyelins accounted for 56 % of total sphingolipids, followed by ceramides at 28 %, hexosylceramides at 15 %, and lactosylceramides at 1 % (**Figure 14B.1**). Consistent with the plasma data, the proportion of sphingomyelins decreased, and the proportion of ceramides increased in GSD Ia mice. The liver tissue samples also exhibited distinct changes in subgroup proportions based on chain length within the sphingomyelins. The proportion of long-chain SM increased from 21 % of total sphingomyelins in WT mice to 34 % in GSD Ia mice, while the proportion of very-long-chain SM decreased from 79 % in WT mice to 66 % in GSD Ia mice (**Figure 14B.2**).

CHAPTER 5. DISCUSSION 1: GSD Ia and NAFLD

With the advancement of dietary therapy and monitoring systems, the prognosis for patients with GSD Ia has been greatly improved. Nonetheless, long-term inflammatory complications still pose a huge burden to both GSD Ia patients and clinicians. In particular, adult patients with GSD Ia face a high risk of morbidity and mortality due to the malignant transformation of adenomas (9, 12). During the last decades, the improvements in life expectancy and quality of life for GSD Ia patients have shifted the focus of clinical treatment and management towards preventing or delaying the progression of long-term complications (7, 9). Metabolic control has been hypothesized to play a major role in the pathophysiology of chronic liver and kidney inflammation, yet the exact aetiology of GSD Ia-HCA development remains poorly understood (1, 7). Given the limited understanding of the pathogenesis of GSD Ia-HCA, we sought to investigate similar liver diseases to explore the underlying mechanisms of liver inflammation in GSD Ia.

Both NAFLD and GSD Ia-HCA involve the buildup of fat and glycogen in hepatocytes, resulting in chronic liver damage and potentially leading to the development of hepatic tumors (69). Traditionally, triglycerides and cholesterol were regarded as the primary lipid markers in HCA. However, recent research has highlighted the involvement of another pro-inflammatory lipid class, namely sphingolipids, in the pathogenesis of metabolic disturbances associated with steatosis (70, 71). The relative obscurity of sphingolipids in the past was due to the challenge of studying this minor lipid class. However, the advent of LC-MS/MS technologies has enabled researchers to investigate sphingolipids with greater accuracy and has led to an increased understanding of their role in metabolic disorders in recent years. In this study, we sought to

identify metabolic similarities by comparing changes in the endogenous sphingolipids in GSD Ia mice to those in NAFLD mice (11, 14, 21).

		Ceramide		Sphingomyelin	
		Long-chain	Very-long-chain	Long-chain	Very-long-chain
Result from this study					
GSD Ia	Mice plasma	Increase	Increase	Increase	Increase
	Mice liver	Increase	Decrease	Decrease	Decrease
Literature Review					
NAFLD	Mice plasma	Increase ^{a,b} (71, 72)	Increase ^{a,b} (71, 72)	Increase ^{c,d} (71, 73)	Increase ^{c,d} (71, 73)
	Mice liver	Increase ^{a,b} (71, 72)	Decrease ^{c,e} (74, 75)	Increase ^{c,d} (73, 76)	Decrease ^{c,e} (74, 75)
HCC	Mice liver	Decrease ^f (76, 77)		Increase ^f (76, 77)	

Table 7. Sphingolipid perturbation in mouse hepatocytes: a comparison between GSD Ia and NAFLD

Footnotes in the table provide additional information about the methodologies used for determining the results – ^a: Lipid analysis by LC-MS/MS, ^b: SMase activity assay, ^c: lipid analysis, ^d: SPT activity assay, ^e: gene expression analysis, ^f: lipid analysis by LC-QTOF MS

Our study identified that the liver of GSD Ia mice exhibits a disruption in the acyl chain specificity of ceramide species: an increase in long-chain ceramides and a decrease in very-long-chain ceramides (**Table 7**). This unique pattern has been commonly observed in studies of NAFLD (71, 76). A recent review by Hajduch *et al.* highlighted the role of long-chain ceramides in the development of hepatic steatosis and they linked this molecular with the "second hit" of NAFLD, including impaired glucose homeostasis and metabolic deterioration (71). Along with NAFLD studies, this study supports the specific role of long-chain ceramides in pathophysiology and verifies their proapoptotic effects in metabolic diseases. However, it is important to note that most conclusions regarding the cellular functions of sphingolipids' side chain have been drawn from studies on genetic knockout models or from those with increasing ceramide exposure (70,

71, 78). Therefore, the precise physiological roles of ceramide acyl chain lengths are still not fully understood.

While further research is necessary to establish more conclusive findings, some studies have identified particular inflammatory mechanisms that are stimulated by ceramides of specific chain lengths (79-81). A study by the Mukhopadhyay *et al.*, highlighted that the direct interaction of ceramide with PP2A is a crucial step in regulating the activity of PP2A (80). Moreover, this ceramide-induced proinflammatory signaling appears to be contingent upon the length of its side chain (80). Specifically, C18 Cer had a higher affinity for binding with the PP2A inhibitor protein compared to other ceramides which subsequently leads to apoptotic consequences including growth inhibition and apoptosis (79, 81). The PKC ζ signaling kinase, an important player in insulin's metabolic actions, has also been linked to ceramides. The exact mechanisms underlying how ceramide interacts with PKC ζ were previously unclear until a study by Dr. Bieberich's team shed light on the subject (82). They have identified the precise location of the ceramide binding domain in PKC ζ , through which they have explained in detail how ceramide, especially C16 Cer, functions as a signaling molecule in the cell membrane (82). To summarize, this available evidence suggests that the inflammatory effects of ceramides are dependent on the length of their side chain, with long-chain ceramides being particularly deleterious in cellular processes (79, 80, 82). It emphasizes the importance of considering the specific structural features of ceramides when studying their biological effects and support the notion that different ceramide species have distinct functional roles in cellular signaling and metabolism.

Another key finding of this study is that the plasma lipidomic profiles are not always reflective of liver metabolism in GSD Ia animal models (**Table 5 & 6**). The plasma samples

from GSD Ia mice presented increased levels of most of the sphingolipids compared to the wild type. On the contrary, the liver from GSD Ia mice showed opposite patterns: decreased levels in sphingomyelins and very-long-chain ceramides. These conflicting outcomes between the organ and fluid are interestingly consistent with the results from recent sphingolipidomic studies on NAFLD mice. During hepatic steatosis, an increase in the plasma ceramide was generally observed in NAFLD mouse models, while none in the liver (25, 27, 71). These divergent data could be explained by the theory that the liver is capable of detecting the intracellular overproduction of ceramide and prevents its accumulation by increasing its secretion via lipoproteins and vesicles (76). In steatohepatitis, the liver is unable to keep up with the intracellular overproduction of sphingolipids, leading to significant accumulation of hepatocyte ceramide within cells (71, 83). Hence, the hepatic ceramide increase becomes conspicuous in the NASH stage (**Table 7**) (70, 83). Not only the excess fat availability but also the sustained inflammation could further provoke the intracellular ceramide production through the activation of sphingomyelinase (11, 29). This vicious cycle may further increase hepatocellular susceptibility to the constant injuries, eventually leading to cirrhosis (71, 83). Although the precise role of sphingolipids in the pathogenesis of NAFLD has not been clearly explored yet, many studies have exhibited that sphingolipid metabolites significantly impact the hepatic pathophysiology differently along the disease progression (11, 24, 28). Thus, monitoring the sphingolipids across the broad stages of GSD Ia mice may provide a significant clue to understand the pathogenesis of GSD Ia-HCA or cirrhosis.

Based on our findings, we recognized that there is a similarity in the sphingolipidomic disruption between early GSD Ia mice and NAFLD mice. This observation suggests a potential shared pathogenesis between GSD Ia and NAFLD during the progression of the disease.

CHAPTER 6. DISCUSSION 2: Sphingolipid profiles

Since the early 2000s, LC-MS/MS has been increasingly utilized in research laboratories, leading to a significant body of research on this technique. One research field that has benefited from LC-MS/MS advancement is the study of sphingolipids (52). The intricate and diverse structural characteristics of sphingolipids posed a significant challenge for the detection and quantification of these species with a high degree of sensitivity and selectivity prior to the development of LC-MS/MS (52, 55, 66). The current trend in LC-MS/MS-based lipidomic studies is to focus on measuring lipid concentration and identifying up and down differences in metabolic diseases. However, our investigation goes beyond this approach by exploring the compositional transition of sphingolipids in GSD Ia mouse models.

In our current study, we analyzed sphingolipid profiles in different fluid and organ of mice models, including plasma and liver tissue. Our findings revealed that sphingolipid profiles vary significantly between two regions. In wild type mice, the plasma was found to be composed of 90 % sphingomyelins, while the liver tissue was found to consist of 56 % sphingomyelins (**Figure 14A.1 & 14B.1**). These observations highlight notable differences between the two regions, which may be informative about the specific roles played by sphingomyelins in different tissue or organs. In plasma, sphingomyelins are primarily present in lipoproteins and they are recognized to contribute to their stability and clearance (84). In contrast, sphingomyelin in liver has been implicated in regulating lipid metabolism, specifically in the formation of lipid droplets which can lead to the development of liver diseases such as HCA and steatohepatitis (21, 25, 76). Therefore, our findings suggest that the distinct roles of sphingolipids may vary depending on the tissue or organ in which it is present, and further studies are needed to fully understand the

functional properties of sphingolipid subgroups in different physiological and pathological conditions.

Our selection of experimental subjects centered on 2-week-old mice, driven by the enduring obstacles posed by the viability of aged mice. As GSD Ia mice advanced in age, their mortality occurred as a consequence of hypoglycemia. For this reason, obtaining older mice that had not undergone any gene therapy proved to be practically challenging. Given that sex differences involve distinct mechanisms related to body fat and lipid intermediates (85), it is important to acknowledge that another limitation of this thesis lies in the insufficient data available to fully explore the influence of sex on sphingolipid profiles. The study conducted by Mulwijk *et al.* highlighted the pronounced sexual dimorphism in sphingolipid alterations across various age groups (86). Their study effectively delineated the shifting pattern of plasma sphingolipid concentrations in correlation with age among both males and females (86). Specifically, the study revealed that young women exhibit lower sphingolipid levels compared to their male counterparts. However, the rate of sphingolipid increase with age is significantly more rapid in women than in men. Consequently, this age-associated disparity culminates in higher sphingolipid concentrations among women, particularly in advanced age (86). While the precise underpinnings of these disparities in sphingolipidomic metabolic processes between sexes remain to be elucidated, investigating the robustness of the associations between sex, age, and sphingolipid profiles holds significant promise for prospective research endeavors.

Recent studies have emphasized the pivotal role of sphingolipid metabolism enzymes in regulating the delicate balance of sphingolipids in cells (22, 87). These enzymes have been found to employ several mechanisms that are specific to different organelles, underscoring the complexity of sphingolipid metabolism regulation (22). Hence, incorporating enzyme

measurements in conjunction with sphingolipid quantification would offer a more comprehensive understanding of sphingolipid metabolism and its intricate regulatory mechanisms.

Although the absolute levels of sphingolipids were highly increased across all species in GSD Ia mice plasma, the composition of subgroups was significantly distorted in the GSD Ia group compared to the wild type (**Figure 14A & Table 5**). Our study has uncovered reciprocal changes between ceramides and sphingomyelins in the plasma of GSD Ia mice, representing a significant breakthrough in our understanding of sphingolipid metabolism. Previous research has suggested that changes in the circulating ceramide levels can have significant effects on the functional properties of lipoproteins, influencing their metabolism, insulin signaling, and inflammation (25, 42, 84). Thus, the observed increase in specific sphingolipid subgroups within the plasma of GSD Ia mice may have important implications for the physiological function of different sphingolipids and their potential role in the progression of GSD Ia.

To sum up, this study not only provides important insights into the compositional transition of sphingolipids in GSD Ia pathogenesis, but also provides new avenue for exploring the potential effects of sphingolipid alterations on lipid metabolism and lipoprotein function within this population.

CHAPTER 7. FUTURE DIRECTIONS

7.1 Sphingolipids changeover along the GSD Ia progression

This study provides evidence of sphingolipid perturbation in individuals with GSD Ia. However, the causal relationship between sphingolipid perturbation and liver inflammation in GSD Ia cannot be established with this study alone. Further analysis of sphingolipids in mice with GSD Ia at various ages may shed light on the changes in sphingolipid profiles throughout the progression of the disease phenotype.

Recent studies have well established the transition in sphingolipid metabolism across different stages of NAFLD (**Table 7**) (76). In steatosis, the pro-inflammatory species, ceramides, were primarily elevated in hepatocyte which in turn resulted in specific symptoms such as insulin resistance and mitochondrial dysfunction (76, 83). However, in carcinoma, ceramides were markedly decreased in liver tissues, while other proliferative species, particularly S1P, were increased to promote a favorable environment for tumor growth (83). In light of these findings, our study demonstrated that early GSD Ia mice exhibit a comparable disturbance of hepatocyte sphingolipid metabolism to that observed in the early stage of NAFLD mice.

There was also a unique pattern of sphingolipid changeover in GSD Ia mice that has not been previously reported in cases of NAFLD. In NAFLD studies, they observed that sphingomyelin also had a chain length specific changeover like ceramide: long-chain SM species were increased in NAFLD mice, and very-long-chain SM were decreased (71). However, GSD Ia mice exhibited that all sphingomyelins, including both long-chain and very-long-chain SM, were decreased in hepatocyte compared to the wild type (**Table 6 & 7**). Do these differences

suggest specific inflammation mechanisms that are unique to GSD Ia? At present, this remains unknown. However, this would be an interesting topic for further investigation.

7.2 Sphingolipids changeover in GSD Ia-kidneys

Kidneys are also susceptible organs in GSD Ia due to the deposition of glycogen and fat (9). This study has shown the sphingolipid perturbations in the liver tissue of a GSD Ia mouse model which may be linked to endogenous lipid overproduction and inflammation. Therefore, it would be valuable to investigate whether GSD Ia kidneys exhibit sphingolipidomic alterations, and if so, whether the affected organs, the liver and kidneys, display similar or distinct sphingolipidomic patterns.

Several studies have highlighted the metabolic link between kidney inflammation in GSD Ia and diabetic kidney diseases (DKD) (88). Clinical manifestations of kidney inflammation typically include excessive urination and dehydration, followed by persistent albuminuria (> 300 mg/24 h or > 300 mg/g creatinine) and a progressive decline in glomerular filtration rate (GFR) (< 60 GFR), which can lead to kidney failure (89). Patients with GSD Ia experience a similar progression of clinical kidney symptoms as illustrated above (90). A study by Rajas *et al.* established a novel illustration of the metabolic similarities between GSD Ia and DKD and highlighted that both are characterized by abnormal lipid metabolism (88). Recent studies have reported sphingolipid changes in DKD patients and animal models (91). Notably, urinary ceramide levels were observed to increase from stage 1 to DKD patients, and in stage 4, which is indicative of severe clinical phenotypes of DKD, the ceramide levels suddenly dropped (88, 91). This suggests that ceramides may play a role as inflammatory inducers in the pathogenesis of kidney diseases. Hence, it would be intriguing to explore whether patients with GSD Ia share

similar sphingolipidomic profiles with individuals affected by DKD, as a growing body of literature has suggested the existence of metabolic similarities between these disorders.

7.3 Pharmacological interventions in sphingolipid metabolism

Nowadays, there are FDA-approved drugs that directly interact with sphingolipid-metabolizing enzymes and modulate related pathways, such as myriocin and fingolimod.

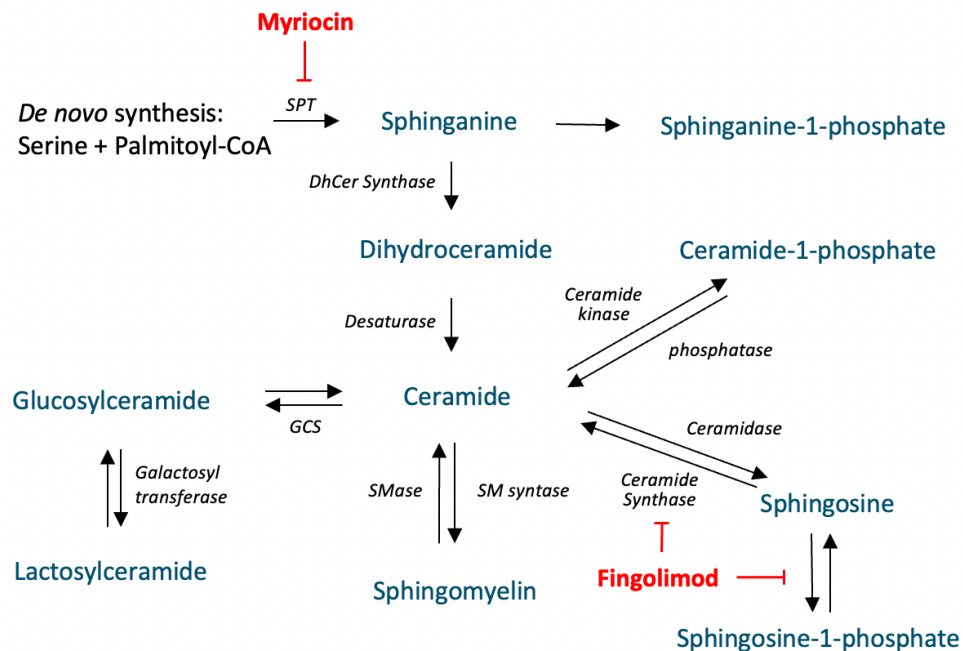


Figure 15. FDA-approved drugs targeting sphingolipid metabolizing enzymes.

Myriocin, a specific inhibitor of sphingolipid *de novo* synthesis, has been extensively used both *in vitro* and *in vivo* in several animal studies (**Figure 15**) (92, 93). Particularly, Myriocin-treated mice demonstrated reduced ceramide levels due to the drug's inhibition of biosynthesis, which resulted in clinical improvements in hepatic insulin resistance and oxidative

stress (93). These effects consequently contributed to the amelioration of steatosis in NAFLD or obese mice (92).

Fingolimod is an immunomodulating medication that interferes with sphingosine kinase 2 activity and inhibits ceramide synthesis (**Figure 15**) (94). A recent study by Rohrbach *et al.*, has demonstrated that Fingolimod is effective in treating murine models of NAFLD (95). The study found that oral administration of Fingolimod to NAFLD mice significantly improved glucose tolerance and reduced hepatocyte lipid accumulation. This, in turn, helped ameliorate the progression of steatosis (95).

Although the exact mechanisms are unknown, certain medications also exhibited the ability to induce alterations in endogenous sphingolipid levels (96, 97). One such medication is fenofibrate, an FDA-approved oral drug widely used to treat patients with hypertriglyceridemia, hypercholesterolemia, or mixed dyslipidemia (96). Recent study by Croyal *et al.* has confirmed that fenofibrate-treated T2D patients experienced a global decrease in plasma ceramides (96). Given that fenofibrate acts on lipoprotein metabolism, the study suggested that the ceramide reduction could be related to accelerated lipoprotein secretion and/or catabolism (96). Fenofibrate is also occasionally used for GSD Ia patients in case they have severe hepatic lipid and glycogen accumulation (97). Therefore, it would be intriguing to investigate whether fenofibrate has clinical benefits in GSD Ia patients, such as lowering ceramide levels and preventing hepatic adenomas.

These promising outcomes with sphingolipid-related medications in reducing ceramide levels raise the question of their potential clinical benefits to patients with GSD Ia, particularly in ameliorating chronic liver inflammation. Further investigation would be necessary to determine the therapeutic potential of these drugs in the treatment of GSD Ia complications.

CHAPTER 8. CONCLUSION

In the early 1980s, uncooked cornstarch emerged as a therapeutic option for GSD I and still remains the primary treatment approach to date (98). While this treatment has significantly improved the metabolic derangement in GSD Ia, long-term complications still afflict many patients. One of the significant challenges in preventing such complications is the limited comprehension of the mechanisms underlying chronic inflammation in GSD Ia, which hinders the development of effective interventions. Therefore, the primary objective of this study was to investigate whether sphingolipidomic mechanisms play a role in the susceptibility to hepatic adenoma and other long-term complications in individuals with GSD Ia.

Sphingolipid metabolism is a relatively new area in metabolomic studies, largely due to the challenges associated with measuring these complex and diverse molecules, as well as their low abundance in biological samples. However, recent advancements in analytical techniques, such as LC-MS/MS, have enabled the simultaneous quantification of sphingolipids with high sensitivity and selectivity. Despite these advancements, few studies have explored the sphingolipid metabolism in GSD Ia. Hence, our study represents the first attempt to provide a semi-comprehensive overview of sphingolipid profiles in GSD Ia animal models using LC-MS/MS.

In this thesis, we have shown the comparison and contrast of endogenous sphingolipid changeover between GSD Ia and NAFLD mice. This approach is crucial for gaining a deeper understanding of the liver complications in GSD Ia. Building on the existing knowledge that sphingolipids play a significant role in NAFLD as lipotoxic mediators, our research has revealed

that GSD Ia animals display anomalous sphingolipid metabolism in both plasma and liver tissues, potentially establishing a link to the pathophysiological similarities with NAFLD.

Specimens are commonly used in clinical and research laboratories as an easy way to obtain samples for biochemical analysis (99). However, our research raises fundamental questions about whether blood can be used as a surrogate marker to reflect the liver sphingolipidome in GSD Ia. While several studies have illustrated the relationship of sphingolipid changeover between plasma and liver, there are still many possibilities for misinterpreting the results (99). For example, elevated plasma ceramide levels are often attributed to increased excretion from the liver in NAFLD mice, but there could be other reasons for elevated blood levels of ceramide, such as cardiovascular events or dietary sphingolipids (21, 25, 36). Therefore, caution should be exercised when using plasma as a biomarker to study the liver sphingolipidome in GSD Ia or other metabolic disorders. Moreover, further research is needed to clarify the relationship between plasma and liver sphingolipids, and to determine the most accurate methods for assessing sphingolipid metabolism in both plasma and liver. This will be critical for improving our understanding of the involvement of sphingolipids in the pathogenesis of chronic liver inflammation and for developing effective therapeutic strategies.

Numerous studies on sphingolipid metabolites focus on the quantification and comparing levels of species. However, our study aimed to elucidate overall trends in sphingolipid profiles through compositional analysis. Our approach was validated by discovering significant shifts in ceramide and sphingomyelin proportions in GSD Ia. These shifts were not limited to the subgroup distributions, but they were also observed between different chain length species. These findings demonstrate the value of compositional analysis in understanding the

sphingolipid metabolism in GSD Ia and underscore the need further research into the functional implications of these alterations.

This study represents a promising starting point for future research on sphingolipid metabolism in GSD Ia. Our findings provide evidence of significant sphingolipidomic imbalances in GSD Ia animal models, which have the potential to serve as triggers for the progression of chronic inflammation in GSD Ia. Moving forward, there is ample opportunity to further investigate the mechanisms underlying these sphingolipid perturbations, as well as their downstream effects on metabolic pathways and disease progression. Our ultimate hope is that this study will stimulate further research in this area, thereby enhancing our comprehension of the underlying mechanisms of GSD Ia, and consequently, mitigating the burden of long-term complications for patients with this disorder.

References

1. Kishnani PS, Austin SL, Abdenur JE, Arn P, Bali DS, Boney A, et al. Diagnosis and management of glycogen storage disease type I: a practice guideline of the American College of Medical Genetics and Genomics. *Genet Med*. 2014;16(11):e1.
2. Özen H. Glycogen storage diseases: new perspectives. *World journal of gastroenterology: WJG*. 2007;13(18):2541.
3. Wolfsdorf JI, Weinstein DA. Glycogen storage diseases. *Reviews in Endocrine and Metabolic Disorders*. 2003;4:95-102.
4. Wolfsdorf JI, Holm IA, Weinstein DA. Glycogen storage diseases. Phenotypic, genetic, and biochemical characteristics, and therapy. *Endocrinol Metab Clin North Am*. 1999;28(4):801-23.
5. Bandsma RH, Smit GP, Kuipers F. Disturbed lipid metabolism in glycogen storage disease type 1. *Eur J Pediatr*. 2002;161 Suppl 1:S65-9.
6. Franco LM, Krishnamurthy V, Bali D, Weinstein DA, Arn P, Clary B, et al. Hepatocellular carcinoma in glycogen storage disease type Ia: A case series. *Journal of Inherited Metabolic Disease*. 2005;28(2):153-62.
7. Moest W, van der Deure W, Koster T, Spee-Dropková M, Swart-Busscher L, de Haas RJ, et al. Glycogen storage disease type Ia: Adult presentation with microcytic anemia and liver adenomas. *Hepatology*. 2018;68(2):780-2.
8. Rake JP, Visser G, Labrune P, Leonard JV, Ullrich K, Smit GP. Glycogen storage disease type I: diagnosis, management, clinical course and outcome. Results of the European Study on Glycogen Storage Disease Type I (ESGSD I). *Eur J Pediatr*. 2002;161 Suppl 1:S20-34.
9. Fernandes J, Saudubray J-M, Van den Berghe G, Walter JH. *Inborn metabolic diseases: diagnosis and treatment: Springer Science & Business Media; 2006.*
10. Ross KM, Ferrecchia IA, Dahlberg KR, Dambaska M, Ryan PT, Weinstein DA. Dietary Management of the Glycogen Storage Diseases: Evolution of Treatment and Ongoing Controversies. *Adv Nutr*. 2020;11(2):439-46.
11. Calderaro J, Labrune P, Morcrette G, Rebouissou S, Franco D, Prévot S, et al. Molecular characterization of hepatocellular adenomas developed in patients with glycogen storage disease type I. *J Hepatol*. 2013;58(2):350-7.
12. Jang HJ, Yang HR, Ko JS, Moon JS, Chang JY, Seo JK. Development of Hepatocellular Carcinoma in Patients with Glycogen Storage Disease: a Single Center Retrospective Study. *J Korean Med Sci*. 2020;35(1):e5.
13. Reddy SK, Kishnani PS, Sullivan JA, Koeberl DD, Desai DM, Skinner MA, et al. Resection of hepatocellular adenoma in patients with glycogen storage disease type Ia. *Journal of hepatology*. 2007;47(5):658-63.
14. Dambaska M, Labrador EB, Kuo CL, Weinstein DA. Prevention of complications in glycogen storage disease type Ia with optimization of metabolic control. *Pediatr Diabetes*. 2017;18(5):327-31.
15. Wang DQ, Fiske LM, Carreras CT, Weinstein DA. Natural history of hepatocellular adenoma formation in glycogen storage disease type I. *J Pediatr*. 2011;159(3):442-6.
16. Di Rocco M, Calevo MG, Taro M, Melis D, Allegri AE, Parenti G. Hepatocellular adenoma and metabolic balance in patients with type Ia glycogen storage disease. *Mol Genet Metab*. 2008;93(4):398-402.

17. Beyzaei Z, Geramizadeh B, Karimzadeh S. Diagnosis of hepatic glycogen storage disease patients with overlapping clinical symptoms by massively parallel sequencing: a systematic review of literature. *Orphanet J Rare Dis.* 2020;15(1):286.
18. Levy M, Futerman AH. Mammalian ceramide synthases. *IUBMB life.* 2010;62(5):347-56.
19. Bartke N, Hannun YA. Bioactive sphingolipids: metabolism and function. *Journal of lipid research.* 2009;50:S91-S6.
20. Gulbins E, Li PL. Physiological and pathophysiological aspects of ceramide. *American Journal of Physiology-Regulatory, Integrative and Comparative Physiology.* 2006;290(1):R11-R26.
21. Maceyka M, Spiegel S. Sphingolipid metabolites in inflammatory disease. *Nature.* 2014;510(7503):58-67.
22. Hussain MM, Jin W, Jiang X-C. Mechanisms involved in cellular ceramide homeostasis. *Nutrition & Metabolism.* 2012;9(1):71.
23. Codini M, Garcia-Gil M, Albi E. Cholesterol and Sphingolipid Enriched Lipid Rafts as Therapeutic Targets in Cancer. *Int J Mol Sci.* 2021;22(2).
24. Pitson SM. Regulation of sphingosine kinase and sphingolipid signaling. *Trends Biochem Sci.* 2011;36(2):97-107.
25. Iqbal J, Walsh MT, Hammad SM, Hussain MM. Sphingolipids and Lipoproteins in Health and Metabolic Disorders. *Trends Endocrinol Metab.* 2017;28(7):506-18.
26. Le Barz M, Boulet MM, Calzada C, Cheillan D, Michalski M-C. Alterations of endogenous sphingolipid metabolism in cardiometabolic diseases: Towards novel therapeutic approaches. *Biochimie.* 2020;169:133-43.
27. Bladergroen BA, Beynen AC, Geelen MJH. Dietary Pectin Lowers Sphingomyelin Concentration in VLDL and Raises Hepatic Sphingomyelinase Activity in Rats 1,2. *The Journal of Nutrition.* 1999;129(3):628-33.
28. Yatomi Y. Plasma sphingosine 1-phosphate metabolism and analysis. *Biochimica et Biophysica Acta (BBA)-General Subjects.* 2008;1780(3):606-11.
29. Hammad SM, Pierce JS, Soodavar F, Smith KJ, Al Gadban MM, Rembiesa B, et al. Blood sphingolipidomics in healthy humans: impact of sample collection methodology. *J Lipid Res.* 2010;51(10):3074-87.
30. Young SA, Mina JG, Denny PW, Smith TK. Sphingolipid and ceramide homeostasis: potential therapeutic targets. *Biochem Res Int.* 2012;2012:248135.
31. Morales A, Lee H, Goñi FM, Kolesnick R, Fernandez-Checa JC. Sphingolipids and cell death. *Apoptosis.* 2007;12(5):923-39.
32. Siskind LJ. Mitochondrial ceramide and the induction of apoptosis. *J Bioenerg Biomembr.* 2005;37(3):143-53.
33. Zigdon H, Kogot-Levin A, Park JW, Goldschmidt R, Kelly S, Merrill AH, Jr., et al. Ablation of ceramide synthase 2 causes chronic oxidative stress due to disruption of the mitochondrial respiratory chain. *J Biol Chem.* 2013;288(7):4947-56.
34. Choi RH, Tatum SM, Symons JD, Summers SA, Holland WL. Ceramides and other sphingolipids as drivers of cardiovascular disease. *Nat Rev Cardiol.* 2021;18(10):701-11.
35. Kikas P, Chalikias G, Tziakas D. Cardiovascular Implications of Sphingomyelin Presence in Biological Membranes. *Eur Cardiol.* 2018;13(1):42-5.
36. Shu H, Peng Y, Hang W, Li N, Zhou N, Wang DW. Emerging Roles of Ceramide in Cardiovascular Diseases. *Aging Dis.* 2022;13(1):232-45.

37. Gencer B, Morrow DA, Braunwald E, Goodrich EL, Hilvo M, Kauhanen D, et al. Plasma ceramide and phospholipid-based risk score and the risk of cardiovascular death in patients after acute coronary syndrome. *Eur J Prev Cardiol.* 2022;29(6):895-902.
38. Chaurasia B, Tippetts TS, Mayoral Monibas R, Liu J, Li Y, Wang L, et al. Targeting a ceramide double bond improves insulin resistance and hepatic steatosis. *Science.* 2019;365(6451):386-92.
39. Poss AM, Krick B, Maschek JA, Haaland B, Cox JE, Karra P, et al. Following Roux-en-Y gastric bypass surgery, serum ceramides demarcate patients that will fail to achieve normoglycemia and diabetes remission. *Med.* 2022;3(7):452-67.e4.
40. Hajduch E, Le Stunff H. Serum ceramides could predict durable diabetes remission following gastric bypass surgery. *Med.* 2022;3(7):440-1.
41. Nikolova-Karakashian M. Alcoholic and non-alcoholic fatty liver disease: Focus on ceramide. *Adv Biol Regul.* 2018;70:40-50.
42. Pagadala M, Kasumov T, McCullough AJ, Zein NN, Kirwan JP. Role of ceramides in nonalcoholic fatty liver disease. *Trends Endocrinol Metab.* 2012;23(8):365-71.
43. Watt MJ, Barnett AC, Bruce CR, Schenk S, Horowitz JF, Hoy AJ. Regulation of plasma ceramide levels with fatty acid oversupply: evidence that the liver detects and secretes de novo synthesised ceramide. *Diabetologia.* 2012;55(10):2741-6.
44. Hornemann T, Alecu I, Hagenbuch N, Zhakupova A, Cremonesi A, Gautschi M, et al. Disturbed sphingolipid metabolism with elevated 1-deoxysphingolipids in glycogen storage disease type I - A link to metabolic control. *Mol Genet Metab.* 2018;125(1-2):73-8.
45. Tran D, Myers S, McGowan C, Henstridge D, Eri R, Sonda S, et al. 1-Deoxysphingolipids, Early Predictors of Type 2 Diabetes, Compromise the Functionality of Skeletal Myoblasts. *Frontiers in Endocrinology.* 2021;12.
46. Weyler J, Verrijken A, Hornemann T, Vonghia L, Dirinck E, von Eckardstein A, et al. Association of 1-deoxy-sphingolipids with steatosis but not steatohepatitis nor fibrosis in non-alcoholic fatty liver disease. *Acta Diabetol.* 2021;58(3):319-27.
47. Zuellig RA, Hornemann T, Othman A, Hehl AB, Bode H, Güntert T, et al. Deoxysphingolipids, novel biomarkers for type 2 diabetes, are cytotoxic for insulin-producing cells. *Diabetes.* 2014;63(4):1326-39.
48. De Hoffmann E, Stroobant V. *Mass spectrometry: principles and applications*: John Wiley & Sons; 2007.
49. Niessen WM. *Liquid chromatography-mass spectrometry*: CRC press; 2006.
50. Matuszewski BK, Constanzer ML, Chavez-Eng CM. Strategies for the assessment of matrix effect in quantitative bioanalytical methods based on HPLC-MS/MS. *Anal Chem.* 2003;75(13):3019-30.
51. Merrill Jr AH, Sullards MC, Allegood JC, Kelly S, Wang E. Sphingolipidomics: high-throughput, structure-specific, and quantitative analysis of sphingolipids by liquid chromatography tandem mass spectrometry. *Methods.* 2005;36(2):207-24.
52. Sullards MC, Liu Y, Chen Y, Merrill Jr AH. Analysis of mammalian sphingolipids by liquid chromatography tandem mass spectrometry (LC-MS/MS) and tissue imaging mass spectrometry (TIMS). *Biochimica et Biophysica Acta (BBA)-Molecular and Cell Biology of Lipids.* 2011;1811(11):838-53.
53. Gorrochategui E, Jaumot J, Lacorte S, Tauler R. Data analysis strategies for targeted and untargeted LC-MS metabolomic studies: Overview and workflow. *TrAC Trends in Analytical Chemistry.* 2016;82:425-42.

54. Tugizimana F, Steenkamp PA, Piater LA, Dubery IA. Conversation on data mining strategies in LC-MS untargeted metabolomics: pre-processing and pre-treatment steps. 2016.
55. van den Ouweland JM, Kema IP. The role of liquid chromatography–tandem mass spectrometry in the clinical laboratory. *Journal of chromatography B*. 2012;883:18-32.
56. McHale KJ. Development of liquid chromatography tandem mass spectrometry instrumentation and methodology for the investigation of biologically active compounds: University of Florida; 2002.
57. Sullards MC, Allegood JC, Kelly S, Wang E, Haynes CA, Park H, et al. Structure-Specific, quantitative methods for analysis of sphingolipids by liquid Chromatography–Tandem mass spectrometry:“Inside-Out” sphingolipidomics. *Methods in enzymology*. 2007;432:83-115.
58. Wu Z, Shon JC, Liu KH. Mass Spectrometry-based Lipidomics and Its Application to Biomedical Research. *J Lifestyle Med*. 2014;4(1):17-33.
59. Hoffmann B, Münch S, Schwägele F, Neusüß C, Jira W. A sensitive HPLC-MS/MS screening method for the simultaneous detection of lupine, pea, and soy proteins in meat products. *Food Control*. 2017;71:200-9.
60. Bielawski J, Pierce JS, Snider J, Rembiesa B, Szulc ZM, Bielawska A. Sphingolipid analysis by high performance liquid chromatography-tandem mass spectrometry (HPLC-MS/MS). *Sphingolipids as Signaling and Regulatory Molecules*. 2010:46-59.
61. Lei KJ, Chen H, Pan CJ, Ward JM, Mosinger B, Jr., Lee EJ, et al. Glucose-6-phosphatase dependent substrate transport in the glycogen storage disease type-1a mouse. *Nat Genet*. 1996;13(2):203-9.
62. FDA. Analytical Procedures and Methods Validation for Drugs and Biologics - Guidance for Industry. U.S. Department of Health and Human Services; 2015.
63. Frej C, Andersson A, Larsson B, Guo LJ, Norström E, Happonen KE, et al. Quantification of sphingosine 1-phosphate by validated LC-MS/MS method revealing strong correlation with apolipoprotein M in plasma but not in serum due to platelet activation during blood coagulation. *Anal Bioanal Chem*. 2015;407(28):8533-42.
64. Liang S, Bian X, Ma J, Arogunjo M, Deorukhkar AA, Krishnan S, et al. Development and validation of a sensitive LC/MS/MS method for the determination of γ -tocotrienol in rat plasma: application to pharmacokinetic studies. *Biomed Chromatogr*. 2013;27(1):58-66.
65. Basit A, Piomelli D, Armirotti A. Rapid evaluation of 25 key sphingolipids and phosphosphingolipids in human plasma by LC-MS/MS. *Anal Bioanal Chem*. 2015;407(17):5189-98.
66. Xu Y, Li H, Han Y, Wang T, Wang Y, Gong J, et al. A simple and rapid method for extraction and measurement of circulating sphingolipids using LC-MS/MS: a targeted lipidomic analysis. *Anal Bioanal Chem*. 2022;414(6):2041-54.
67. Fan H, Feiyang C, Michael SD, Kshemaka G, Ali T, Jonas D, et al. Disrupting peroxisomes alters lipid metabolism in melanoma and uncovers a novel therapeutic vulnerability in combination with MAPK-targeted therapies. *bioRxiv*. 2022:2022.10.25.513718.
68. Hall Z, Bond NJ, Ashmore T, Sanders F, Ament Z, Wang X, et al. Lipid zonation and phospholipid remodeling in nonalcoholic fatty liver disease. *Hepatology*. 2017;65(4):1165-80.
69. Allende DS, Gawrieh S, Cummings OW, Belt P, Wilson L, Van Natta M, et al. Glycogenesis is common in nonalcoholic fatty liver disease and is independently associated with ballooning, but lower steatosis and lower fibrosis. *Liver International*. 2021;41(5):996-1011.

70. Apostolopoulou M, Gordillo R, Koliaki C, Gancheva S, Jelenik T, De Filippo E, et al. Specific Hepatic Sphingolipids Relate to Insulin Resistance, Oxidative Stress, and Inflammation in Nonalcoholic Steatohepatitis. *Diabetes Care*. 2018;41(6):1235-43.
71. Hajduch E, Lachkar F, Ferré P, Foufelle F. Roles of Ceramides in Non-Alcoholic Fatty Liver Disease. *Journal of Clinical Medicine*. 2021;10(4):792.
72. Cinar R, Godlewski G, Liu J, Tam J, Jourdan T, Mukhopadhyay B, et al. Hepatic cannabinoid-1 receptors mediate diet-induced insulin resistance by increasing de novo synthesis of long-chain ceramides. *Hepatology*. 2014;59(1):143-53.
73. Deevska GM, Rozenova KA, Giltiay NV, Chambers MA, White J, Boyanovsky BB, et al. Acid Sphingomyelinase Deficiency Prevents Diet-induced Hepatic Triacylglycerol Accumulation and Hyperglycemia in Mice. *J Biol Chem*. 2009;284(13):8359-68.
74. Montgomery MK, Brown SHJ, Lim XY, Fiveash CE, Osborne B, Bentley NL, et al. Regulation of glucose homeostasis and insulin action by ceramide acyl-chain length: A beneficial role for very long-chain sphingolipid species. *Biochimica et Biophysica Acta (BBA) - Molecular and Cell Biology of Lipids*. 2016;1861(11):1828-39.
75. Yetukuri L, Katajamaa M, Medina-Gomez G, Seppänen-Laakso T, Vidal-Puig A, Oresic M. Bioinformatics strategies for lipidomics analysis: characterization of obesity related hepatic steatosis. *BMC Syst Biol*. 2007;1:12.
76. Simon J, Ouro A, Ala-Ibanibo L, Presa N, Delgado TC, Martínez-Chantar ML. Sphingolipids in Non-Alcoholic Fatty Liver Disease and Hepatocellular Carcinoma: Ceramide Turnover. *Int J Mol Sci*. 2019;21(1).
77. Longato L, Tong M, Wands JR, de la Monte SM. High fat diet induced hepatic steatosis and insulin resistance: Role of dysregulated ceramide metabolism. *Hepatol Res*. 2012;42(4):412-27.
78. Li Z, Guan M, Lin Y, Cui X, Zhang Y, Zhao Z, et al. Aberrant Lipid Metabolism in Hepatocellular Carcinoma Revealed by Liver Lipidomics. *Int J Mol Sci*. 2017;18(12).
79. Garić D, De Sanctis JB, Shah J, Dumut DC, Radzioch D. Biochemistry of very-long-chain and long-chain ceramides in cystic fibrosis and other diseases: The importance of side chain. *Prog Lipid Res*. 2019;74:130-44.
80. Mukhopadhyay A, Saddoughi SA, Song P, Sultan I, Ponnusamy S, Senkal CE, et al. Direct interaction between the inhibitor 2 and ceramide via sphingolipid-protein binding is involved in the regulation of protein phosphatase 2A activity and signaling. *Faseb j*. 2009;23(3):751-63.
81. Saddoughi SA, Gencer S, Peterson YK, Ward KE, Mukhopadhyay A, Oaks J, et al. Sphingosine analogue drug FTY720 targets I2PP2A/SET and mediates lung tumour suppression via activation of PP2A-RIPK1-dependent necroptosis. *EMBO Mol Med*. 2013;5(1):105-21.
82. Wang G, Krishnamurthy K, Umopathy NS, Verin AD, Bieberich E. The carboxyl-terminal domain of atypical protein kinase Czeta binds to ceramide and regulates junction formation in epithelial cells. *J Biol Chem*. 2009;284(21):14469-75.
83. Gorden DL, Myers DS, Ivanova PT, Fahy E, Maurya MR, Gupta S, et al. Biomarkers of NAFLD progression: a lipidomics approach to an epidemic. *J Lipid Res*. 2015;56(3):722-36.
84. Peter Slotte J. Molecular properties of various structurally defined sphingomyelins -- correlation of structure with function. *Prog Lipid Res*. 2013;52(2):206-19.
85. Varlamov O, Bethea CL, Roberts CT. Sex-Specific Differences in Lipid and Glucose Metabolism. *Frontiers in Endocrinology*. 2015;5.

86. Muilwijk M, Callender N, Goorden S, Vaz FM, van Valkengoed IGM. Sex differences in the association of sphingolipids with age in Dutch and South-Asian Surinamese living in Amsterdam, the Netherlands. *Biol Sex Differ*. 2021;12(1):13.
87. Hannun YA, Obeid LM. Many ceramides. *J Biol Chem*. 2011;286(32):27855-62.
88. Rajas F, Labrune P, Mithieux G. Glycogen storage disease type 1 and diabetes: learning by comparing and contrasting the two disorders. *Diabetes Metab*. 2013;39(5):377-87.
89. Afkarian M, Zelnick LR, Hall YN, Heagerty PJ, Tuttle K, Weiss NS, et al. Clinical Manifestations of Kidney Disease Among US Adults With Diabetes, 1988-2014. *Jama*. 2016;316(6):602-10.
90. Aoun B, Sanjad S, Degheili JA, Barhoumi A, Bassyouni A, Karam PE. Kidney and Metabolic Phenotypes in Glycogen Storage Disease Type-I Patients. *Front Pediatr*. 2020;8:591.
91. Nicholson RJ, Pezzolesi MG, Summers SA. Rotten to the Cortex: Ceramide-Mediated Lipotoxicity in Diabetic Kidney Disease. *Front Endocrinol (Lausanne)*. 2020;11:622692.
92. Hodson AE, Tippetts TS, Bikman BT. Insulin treatment increases myocardial ceramide accumulation and disrupts cardiometabolic function. *Cardiovasc Diabetol*. 2015;14:153.
93. Tanase DM, Gosav EM, Petrov D, Jucan AE, Lacatusu CM, Floria M, et al. Involvement of Ceramides in Non-Alcoholic Fatty Liver Disease (NAFLD) Atherosclerosis (ATS) Development: Mechanisms and Therapeutic Targets. *Diagnostics (Basel)*. 2021;11(11).
94. Strader CR, Pearce CJ, Oberlies NH. Fingolimod (FTY720): a recently approved multiple sclerosis drug based on a fungal secondary metabolite. *J Nat Prod*. 2011;74(4):900-7.
95. Rohrbach TD, Asgharpour A, Maczys MA, Montefusco D, Cowart LA, Bedossa P, et al. FTY720/fingolimod decreases hepatic steatosis and expression of fatty acid synthase in diet-induced nonalcoholic fatty liver disease in mice. *J Lipid Res*. 2019;60(7):1311-22.
96. Croyal M, Kaabia Z, León L, Ramin-Mangata S, Baty T, Fall F, et al. Fenofibrate decreases plasma ceramide in type 2 diabetes patients: A novel marker of CVD? *Diabetes Metab*. 2018;44(2):143-9.
97. Yavarow ZA, Kang HR, Waskowicz LR, Bay BH, Young SP, Yen PM, et al. Fenofibrate rapidly decreases hepatic lipid and glycogen storage in neonatal mice with glycogen storage disease type Ia. *Hum Mol Genet*. 2020;29(2):286-94.
98. Chen YT, Bazzarre CH, Lee MM, Sidbury JB, Coleman RA. Type I glycogen storage disease: nine years of management with cornstarch. *Eur J Pediatr*. 1993;152 Suppl 1:S56-9.
99. Vinnakota KC, Pannala VR, Wall ML, Rahim M, Estes SK, Trenary I, et al. Network Modeling of Liver Metabolism to Predict Plasma Metabolite Changes During Short-Term Fasting in the Laboratory Rat. *Frontiers in Physiology*. 2019;10.

Appendices: Supplemental Information

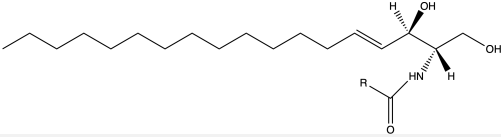
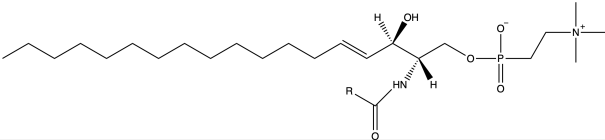
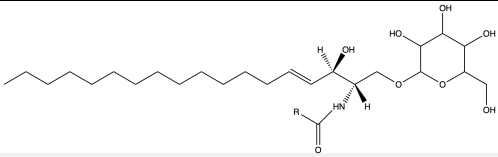
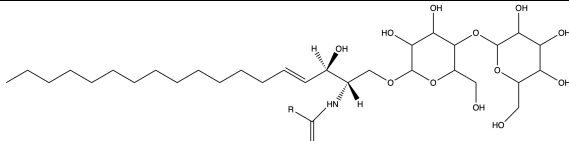
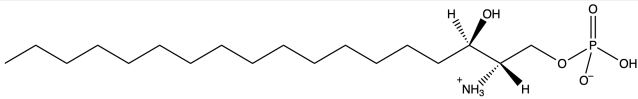
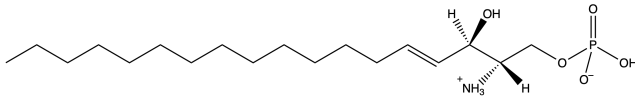
Species		
		
Ceramide	Molecular Formula	Avanti® code
C14 Ceramide (d18:1/14:0)	C ₃₂ H ₆₃ NO ₃	860514
C16 Ceramide (d18:1/16:0)	C ₃₄ H ₆₇ NO ₃	860516
C20 Ceramide (d18:1/20:0)	C ₃₈ H ₇₅ NO ₃	860520
C22 Ceramide (d18:1/22:0)	C ₄₀ H ₇₉ NO ₃	860501
C24 Ceramide (d18:1/24:0)	C ₄₂ H ₈₃ NO ₃	860524
C24:1 Ceramide (d18:1/24:1)	C ₄₂ H ₈₁ NO ₃	860525
		
Sphingomyelin	Molecular Formula	Avanti® code
C16 Sphingomyelin (d18:1/16:0)	C ₃₉ H ₇₉ N ₂ O ₆ P	860584
C16:1 Sphingomyelin (d18:1/16:1)	C ₃₉ H ₇₇ N ₂ O ₆ P	860684
C18 Sphingomyelin (d18:1/18:0)	C ₄₁ H ₈₃ N ₂ O ₆ P	860586
C24 Sphingomyelin (d18:1/24:0)	C ₄₇ H ₉₅ N ₂ O ₆ P	860592
C24:1 Sphingomyelin (d18:1/24:1)	C ₄₇ H ₉₃ N ₂ O ₆ P	860593
		
Lactosyl/Glucosylceramide	Molecular Formula	Avanti® code
C16 Glucosylceramide (d18:1/16:0)	C ₄₀ H ₇₇ NO ₈	860539
C18 Glucosylceramide (d18:1/18:0)	C ₄₂ H ₈₁ NO ₈	860547
C18:1 Glucosylceramide (d18:1/24:0)	C ₄₂ H ₇₉ NO ₈	860548
C24:1 Glucosylceramide (d18:1/24:1)	C ₄₈ H ₉₁ NO ₈	860549
		
C16 Lactosylceramide (d18:1/16:0)	C ₄₆ H ₈₇ NO ₁₃	860576
C18 Lactosylceramide (d18:1/18:0)	C ₄₈ H ₉₁ NO ₁₃	860598
C24 Lactosylceramide (d18:1/24:0)	C ₅₄ H ₁₀₃ NO ₁₃	860577
Sphingolipid-1-phosphate	Molecular Formula	Avanti® code
		
Sphinganine-1-phosphate d18:0	C ₁₈ H ₄₀ NO ₅ P	860536
		
Sphinganine-1-phosphate d18:1	C ₁₈ H ₃₈ NO ₅ P	860492

Table S1. Sphingolipid species information and molecular structure

Reagent	Source	Conc. Stock	Solvent
Internal lipid standards			
C17 Cer d18:1 17:0	Avanti Polar Lipids	0.5 mg/ml	CHCl ₃ :MeOH, 1:1
C17 GlcCer d18:1 17:0	Avanti Polar Lipids	1.25 mg/ml	CHCl ₃ :MeOH, 1:1
d17:0 Sa1P	Avanti Polar Lipids	0.25 mg/ml	MeOH ¹
d17:1 S1P	Avanti Polar Lipids	0.2 mg/ml	MeOH
External lipid standards			
<i>Ceramide</i>			
C14 Cer d18:1 14:0	Avanti Polar Lipids	1.25 mg/ml	CHCl ₃ :MeOH, 1:1
C16 Cer d18:1 16:0	Avanti Polar Lipids	1.25 mg/ml	CHCl ₃ :MeOH, 1:1
C20 Cer d18:1 20:0	Avanti Polar Lipids	1.25 mg/ml	CHCl ₃ :MeOH, 1:1
C22 Cer d18:1 22:0	Avanti Polar Lipids	0.5 mg/ml	CHCl ₃ :MeOH, 3:2
C24 Cer d18:1 24:0	Avanti Polar Lipids	0.5 mg/ml	CHCl ₃ :MeOH, 1:1
C24:1 Cer d18:1 24:1	Avanti Polar Lipids	1.25 mg/ml	CHCl ₃ :MeOH, 1:1
<i>Sphingomyelin</i>			
C16 SM d18:1 16:0	Avanti Polar Lipids	1.25 mg/ml	CHCl ₃ :MeOH, 1:1
C16:1 SM d18:1 16:1	Avanti Polar Lipids	0.5 mg/ml	CHCl ₃ :MeOH, 1:1
C18 SM d18:1 18:0	Avanti Polar Lipids	2.56 mg/ml	CHCl ₃ :MeOH, 1:1
C24 SM d18:1 24:0	Avanti Polar Lipids	2.5 mg/ml	CHCl ₃ :MeOH, 1:1
C24:1 SM d18:1 24:1	Avanti Polar Lipids	1.25 mg/ml	CHCl ₃ :MeOH, 1:1
<i>Glucosylceramide</i>			
C16 GlcCer d18:1 16:0	Avanti Polar Lipids	1.25 mg/ml	CHCl ₃ :MeOH, 1:1
C18 GlcCer d18:1 18:0	Avanti Polar Lipids	1.25 mg/ml	CHCl ₃ :MeOH, 1:1
C18:1 GlcCer d18:1 18:1	Avanti Polar Lipids	1.25 mg/ml	CHCl ₃ :MeOH, 1:1
C24:1 GlcCer d18:1 24:1	Avanti Polar Lipids	0.5 mg/ml	CHCl ₃ :MeOH, 1:1
<i>Lactosylceramide</i>			
C16 LacCer d18:1 16:0	Avanti Polar Lipids	1.25 mg/ml	CHCl ₃ :MeOH, 1:1
C18 LacCer d18:1 18:0	Avanti Polar Lipids	0.5 mg/ml	CHCl ₃ :MeOH, 1:1
C24 LacCer d18:1 24:0	Avanti Polar Lipids	0.5 mg/ml	CHCl ₃ :MeOH, 1:1
<i>Phosphate sphingolipid</i>			
d18:0 Sa1P	Avanti Polar Lipids	0.1 mg/ml	MeOH
d18:1 S1P	Avanti Polar Lipids	0.2 mg/ml	MeOH

Table S2. Lipid standards and stock solutions

¹ If the stock of phosphate sphingolipids is not dissolved in methanol, a small amount of dimethylamine (0.05M to 0.1M) was added to enhance the solubility of the species.

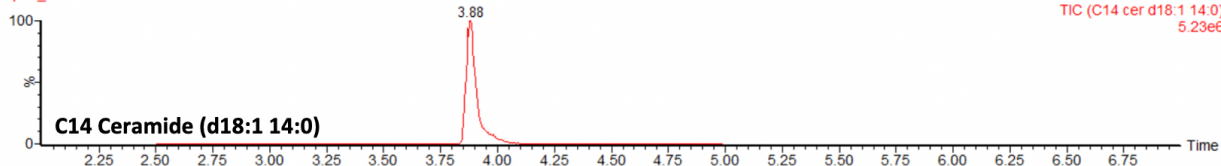
CHCl₃: Chloroform, MeOH: Methanol

A. Ceramide

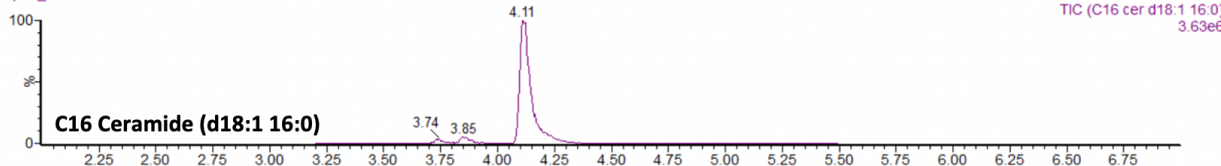
XEVO-TQSmicro#QEE0772

22-Jul-2022 08:14:35

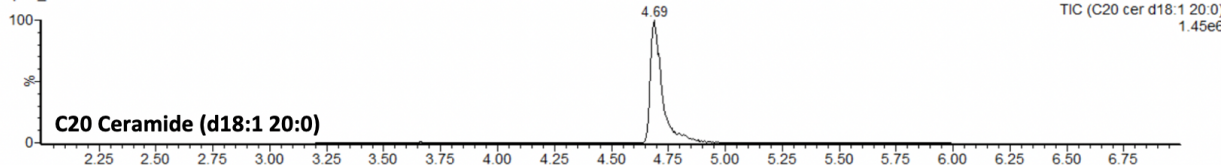
Exp74_cerCalx1



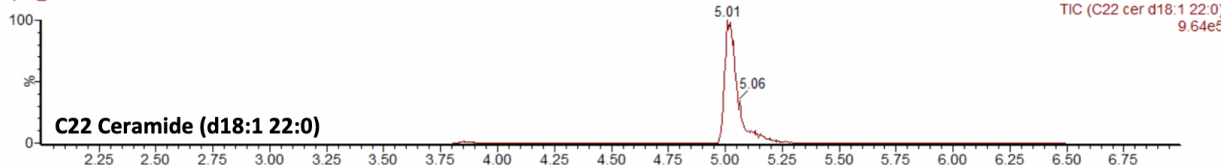
Exp74_cerCalx1



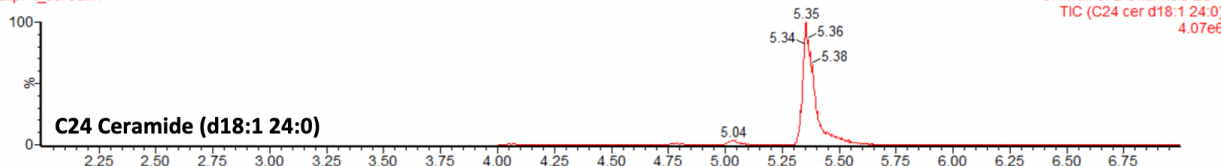
Exp74_cerCalx1



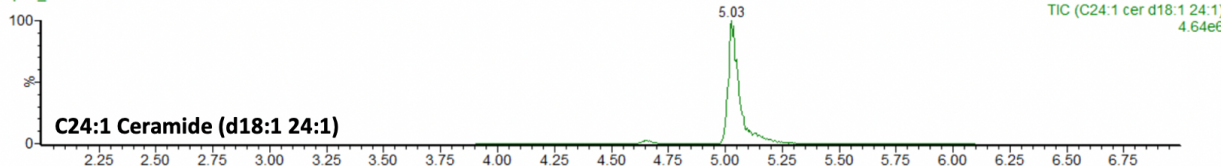
Exp74_cerCalx1



Exp74_cerCalx1



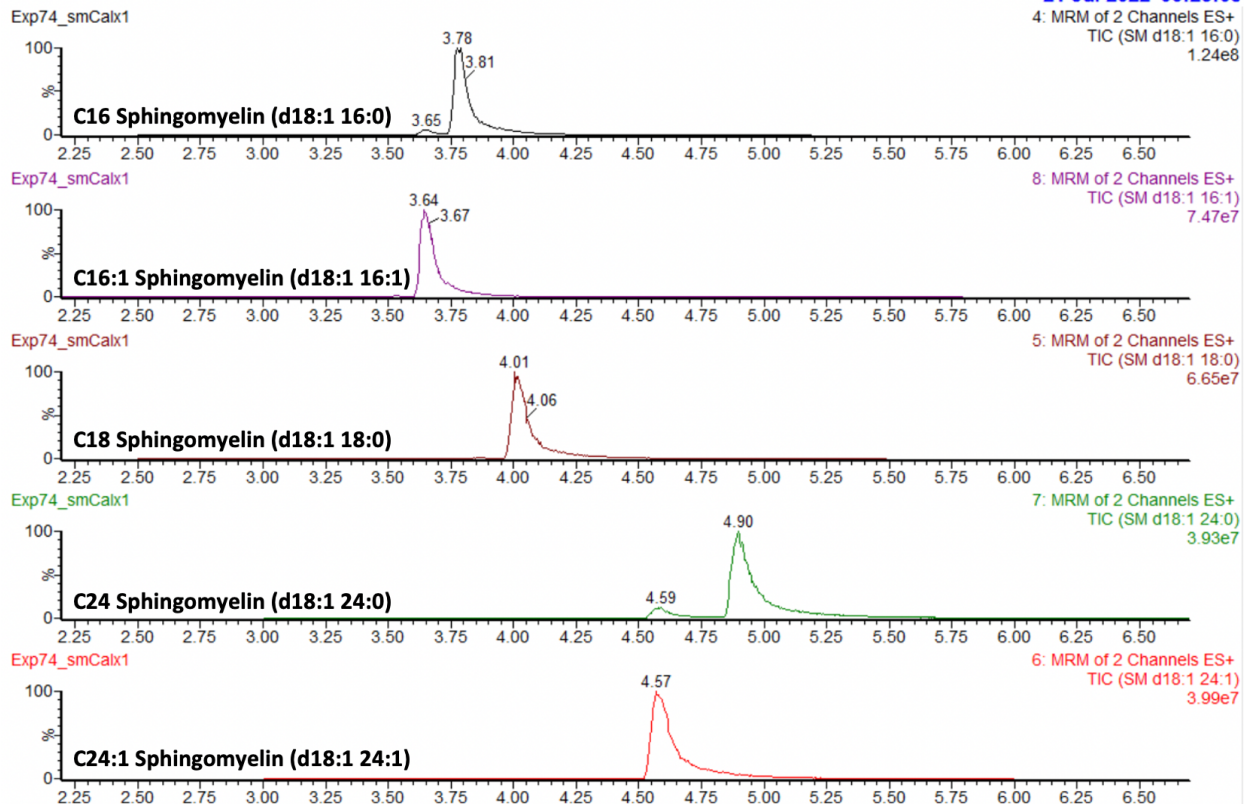
Exp74_cerCalx1



B. Sphingomyelin

XEVO-TQSmicro#QEE0772

21-Jul-2022 06:25:08



C. Complex sphingolipids

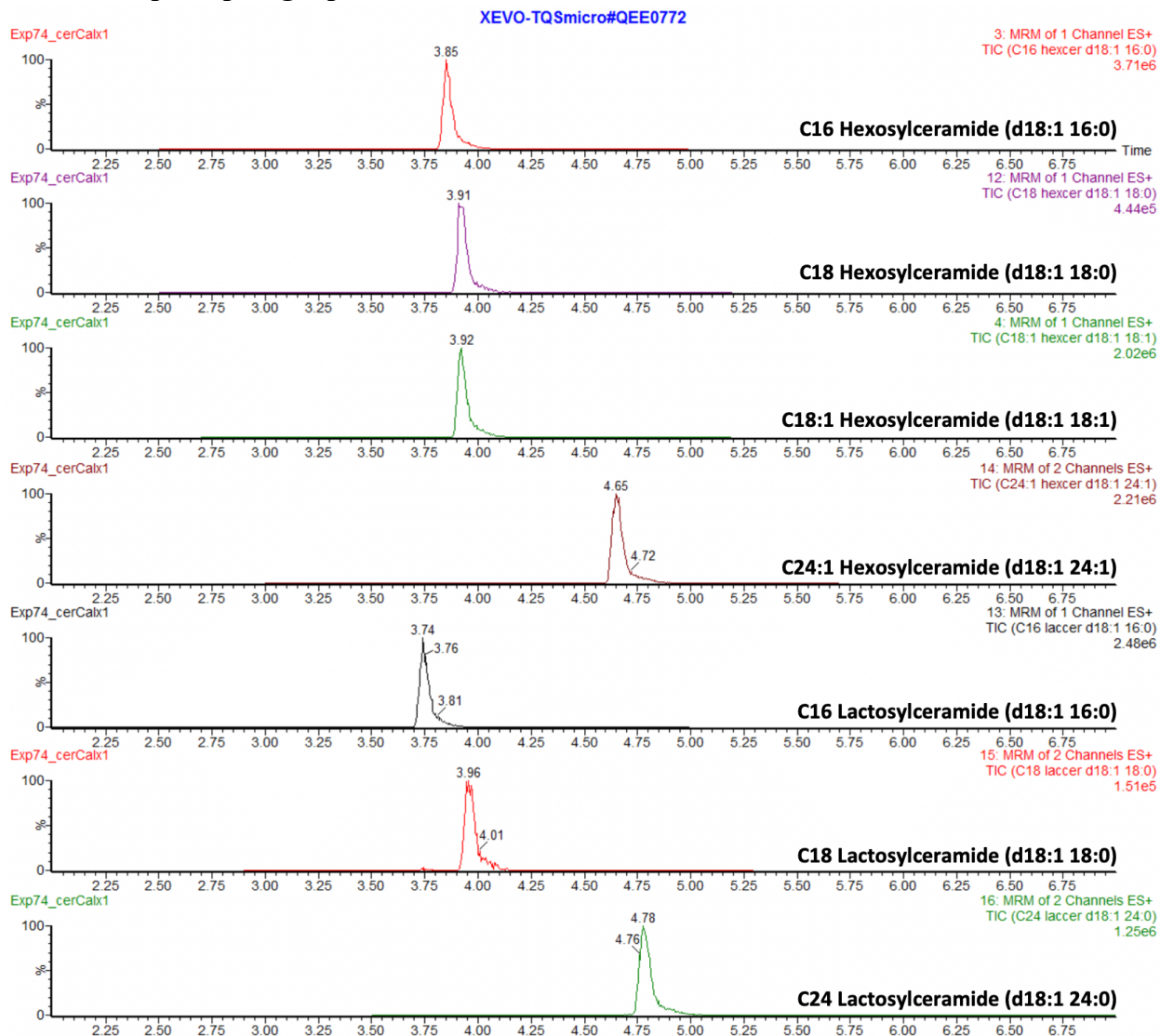


Figure S1. Chromatographic separation of sphingolipids by targeted sphingolipidomics using LC-MS/MS

The numbers marked above the peak indicate the retention time (in minutes) of the corresponding analyte.